学位論文

Development of potent macrocyclic peptide inhibitors against cofactor independent phosphoglycerate mutase of parasitic nematodes

（寄生性線虫コファクター非依存性ホスホグリセリン酸ムターゼに対する大環状ペプチド阻害剤の開発）

平成２８年１０月博士（理学）申請

東京大学大学院理学系研究科
化学専攻余　昊

Abstract

Diseases caused by parasitic nematodes are serious public health problems in developing countries that affect millions of people worldwide. Treatments for parasitic nematode caused diseases, such as the lymphatic filariasis caused by Brugia malayi, have not been well developed to date. The enzyme Cofactor-independent phosphoglycerate mutase (iPGM) catalyzes the critical interconversion of 2-phosphoglycerate and 3-phosphoglycerate in the glycolytic and gluconeogenic metabolic pathways that are essential for the growth of nematodes, implicating iPGM as a potential drug target. However, iPGM is considered as protein with low "druggability", and is thus not suitable for targeting with conventional small molecules. Since small molecules do not have sufficient binding interfaces to interact with the target proteins. Thus, alternative approaches are required for the discovery of iPGM inhibitors, which may be useful in the development of anti-parasite therapies. In this thesis, I report the discovery of macrocyclic peptide inhibitors against iPGMs via the Random non-standard Peptide Integrated Discovery (RaPID) system, Such an approach enables the rapid selection of high affinity iPGM-binders from a genetic code reprogrammed peptide library containing trillions of unique macrocyclic peptides.

In chapter 1, I introduce the situation of infectious diseases caused by parasitic nematodes, such as Lymphatic filariasis and current treatment for these diseases. The limited effective drugs as well as increasing drug resistance call for identification of new drug targets and developing novel drug candidates. Subsequently, the characterization of cofactor-independent phosphoglycerate mutase (iPGM) is described and presents the potential of iPGM as a promising anti-parasite therapeutic target. Then, I discuss the challenges of traditional drug developing methods and introduce advantages of the RaPID system for peptide drug discovery.

In chapter 2, the development of macrocyclic peptides that bind to *B. malayi* iPGM is described as well as the determination of inhibitory activities. Several macrocyclic peptides are identified as *B. malayi* iPGM binders and exhibit inhibitory activity

against iPGM orthologs. Furthermore, the structure activity relationship analysis is carried out on Bm-4 peptides by chemical modifications.

In chapter 3, an attempt at discovering *C. elegans* iPGM inhibitory peptides is discussed. Four macrocyclic peptides were selected and the binding affinity and inhibitory activity are evaluated. Ce-1 and Ce-2 are potent iPGM inhibitor with broad-spectrum inhibitory activity. The binding activity of Ce-2 is further studied via a series of chemical modification, including truncation, substitution and *N*-methylation. The binding site and inhibitory mechanism of macrocyclic peptide is elucidated by obtained co-crystal structure of cyclic peptide and *C. elegans* iPGM complex.

In the last chapter, the achievements in this study were summarized. Briefly, Discovery of such potent, selective, broad spectrum of macrocyclic peptide inhibitors gives new opportunities to develop non-druggable target against infectious nematode species and provide insights for rational drug design in future.

Abbreviations

2-PG	2-phosphoglycerate
3-PG	3-phosphoglycerate
B. malayi	*Brugia malayi*
C. elegans	*Caenorhabditis elegans*
ClAc	*N*-chloroacetyl
DOPA	Dihydroxyphenylananine
D. immitis	*Dirofilaria immitis*
dPGM	Cofactor dependent phosphoglycerate mutase
E. coli	*Escherichia coli*
eFx	Enhanced flexizyme
FIT system	Flexible *in vitro* translation system
HPLC	High performance liquid chromatography
HTS	High throughput screening
IC50	Half maximal inhibitory concentration
iPGM	Cofactor independent phosphoglycerate mutase
LF	Lymphatic filariasis
O. volvulus	*Onchocerca volvulus*
RaPID system	Random non-standard peptide integrated discovery system
RMSD deviation	RMSD deviation
RNAi	RNA interference
RP-HPLC	Reverse-phase HPLC
SPPS	Solid-Phase peptide synthesis
SPR	Surface plasmon resonance

Table of contents

Chapter 1
General introduction

1.1 Infectious parasitic diseases and current treatments

The phylum nematode is an abundant organism in nature, including free-living species and parasitic species infecting plants, animals and humans. Diseases caused by parasitic nematodes have been serious public health problems in developing countries that affect millions of people worldwide.[1,2] Even though these diseases were serious issues in these countries, major pharmaceutical companies had not made sufficient efforts to develop drugs to treat suffering people or protect people, thus so-called neglected diseases.

Lymphatic filariasis (LF) is a tropical infectious disease caused by parasitic nematodes of *Wuchereria bancrofti*, *Brugia malayi*, and *Brugia timori*. This disease is prevalence in tropical countries mainly in Asian and African and has infected over 120 million people worldwide.[3,4] Although LF Infected people are rarely life threatened, LF infection cause significant morbidity or disfigurement leading to permanent and long-term disabilities.[5] River blindness (Onchocerciasis) and heartworm are also infectious diseases caused by parasitic nematodes of *Onchocerca volvulus* and *Dirofilaria immitis,* respectively.[6-10] Mosquito has been known as the intermediate host of parasitic nematodes in which the larval parasites grow into infective larvae and transmit to animal host during a blood meal. The lifespan of parasites is very long, including two weeks in vector and over 5 years in host, indicating the demand of long period drug treatment.

However, the treatment or control methods are insufficient and mainly dependent on annually administration of three chemical drugs: Diethylcarbamazine, Ivermectin and Albendazole. Diethylcarbamazine is the main agent for the treatment of infections and global diseases eliminating programmes, but the action of diethylcarbamazine is not well understood.[11] Recent study has confirmed its effect on arachidonic acid pathway;[12] Ivermectin has been used for onchocerciasis therapy,[13] and results in immobilization of microfilariae by inhibiting glutamate-sensitive channels.[14] Albendazole is another anti-parasite drug with broad-spectrum activity, since this drug affects the formation of microtubule and β-tubulin for parasite development.[15] Nevertheless, traditional therapeutics can only kill immature parasites (microfilarae)

and show little effect on the adult parasites (macrofilarae). [16-18] The adult worms live for a long time in hosts and keep on producing larval parasites. Therefore, eliminating program based on mass drug distribution need to be conducted for years over the life span of adult worms. Eliminating progresses have been observed in many areas, but the increasing of drug resistance becomes an urgent problem, which should be concerned, and also there is continuous demanding for new anti-parasite drugs especially with anti-macrofilarae activity.[19-21]

Table 1-1. The information of parasitic infectious diseases. SSA: sub-Saharan Africa; SEA: Southeast Asia; LA: Latin America

Infection	Causal Agents	Infected population	Area	Treatment	Administration period
Lymphatic filariasis	Wuchereria bancrofti; Brugia malayi; Brugia timori	37 Millions	India, SEA, SSA	Dirthylcarbamazine, Ivermectin and albendazole	5 years
Onchocerciasis	Onchocera volvulus	120 Millions	SSA	Ivermectin	15 years
Heartworm infection	Dirofilaria immitis	—	LA, SEA	Ivermectin, Melarsomine	1.5 years

1.2 iPGM enzyme is a promising drug target for parasitic diseases

The treatments for parasitic diseases are limited by using a small number of chemical molecules. Furthermore, the existing drugs only possess activity against microfilarae (immature parasites) and are less effective on macrofilarae (adult parasites). Therefore long period of drug administration has been highly recommended for eliminating adult worms completely.[8] Thus, the identification of novel anti-parasite therapies and drugs has been demanded to treat and protect people from parasitic infections.

Currently, the genetic and developmental biology of nematodes has been characterized. Genome analysis of *C. elegans* has exploited nematode-specific genes that participate in essential biological processes and are absent in mammal hosts, such as humans.[2,22-24] On the other hand, the whole genome of the filarial parasite *B. malayi* has been analyzed and enables for mining novel drug targets by comparing with the genome of *C. elegans*.[1,25-28] Any proteins or enzymes, which are unique for nematode and involve in metabolic processes, are potential and appropriate targets for development of anti-nematode drugs.[1,29]

Among the identified targets, cofactor independent phosphoglycerate mutases (iPGMs) have been confirmed as crucial metabolic enzyme for the living and development of nematodes and are absent in hosts animals that possess an PGM isozyme of cofactor dependent phosphoglycerate mutase (dPGM) with difference structure and catalytic function.[30,31] The essential character of iPGM has also been tested by RNA interference (RNAi) studies in both nematodes of *C. elegans* and *B. malayi*.[32,33] The results showed that down regulation of iPGM transcript leads to embryonic and larval lethality for *C. elegans*. The RNAi treatment targeting *B. malayi* iPGM resulted in sluggish movement, phenotypic deformities and significant release reduction of microfilarae. These findings demonstrated the importance of iPGM during nematode development and validated iPGM as a promising anti-parasite target.[34,35] The sequence alignment of *C. elegans* and *B. malayi* iPGM showed that they have conserved the catalytic serine residue and other residues that were predicted to be involved in catalytic activity (Figure 1-1).[36-38] The functional similarity of iPGMs

indicates that it is feasible to develop iPGM inhibitors that would have inhibitory activity against target iPGM and be effective against various iPGM enzymes.[39 40]

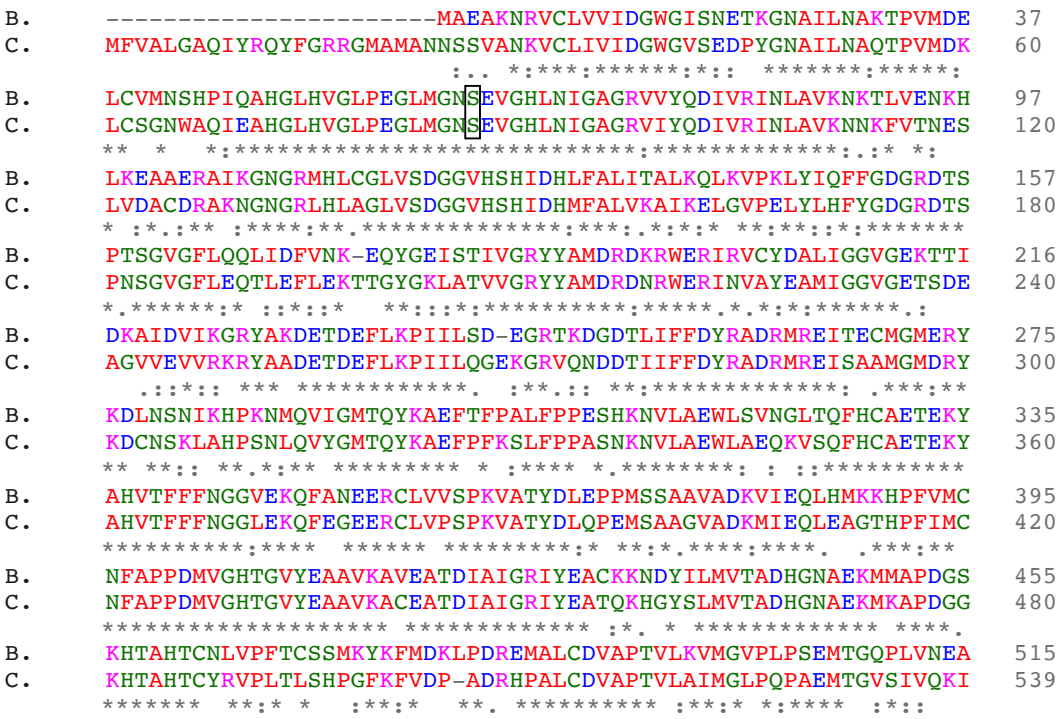

Figure 1-1. Amino acid sequence alignment of *C. elegans* (C.) and *B. malayi* (B.) iPGMs. Catalytic Serine residues are shown in black box.

1.3 Characterization of cofactor independent phosphoglycerate mutase

The phosphoglycerate mutase (PGM) enzymes catalyze the interconversion of 3-phosphoglycerate (3-PG) and 2-phosphoglycerate (2-PG) in the glycolytic and gluconeogenic pathways, which are essential metabolic processes and highly conserved reactions among organisms[41-43] PGMs are classified to two distinct forms, cofactor-independent PGM (iPGM) or cofactor-dependent PGM (dPGM), distinguished on the requirement of cofactor (2,3-diphosphoglycerate). These two enzymes are isozymes and catalyze the same target reaction, but they differ vastly in amino acid sequences, three-dimensional structure and mechanism of catalysis.[41]

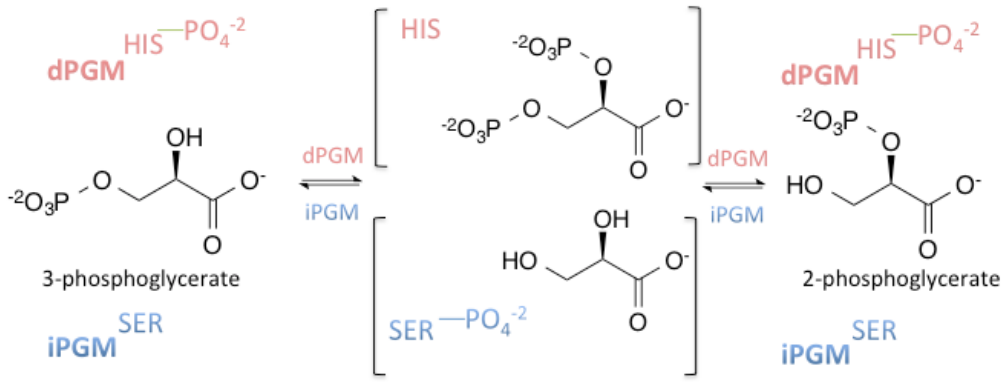

Figure 1-2. PGMs catalyzed interconversion. phosphohistidine intermediate in dPGM (in red) and phosphoserine intermediate in iPGM (in blue).

iPGM is a monomeric enzyme and comprised of ~500 amino acids with a molecular weight of ~50kDa (Figure 1-2).[44] The iPGM enzyme contains two catalytic domains with equal size, a phosphatase domain and a phosphotransferase domain, which interact with each other via surface contacts (Figure 1-3). Its catalytic mechanism has been elucidated as follows: the phosphotransferase catalyzes the transfer of a phosphate group from 3-phosphoglycerate to a serine residue in the active site and form a phosphoserine intermediate, and the phosphate group is transferred back to the glycerate by the phosphotransferase to generate 2-phosphoglycerate (Figure 1-2).[31,45] The iPGM enzyme undergo open-close-open conformation change in catalytic cycle and two domains form an open conformation when the substrate is absent and convert to a closed conformation during catalysis.[46]

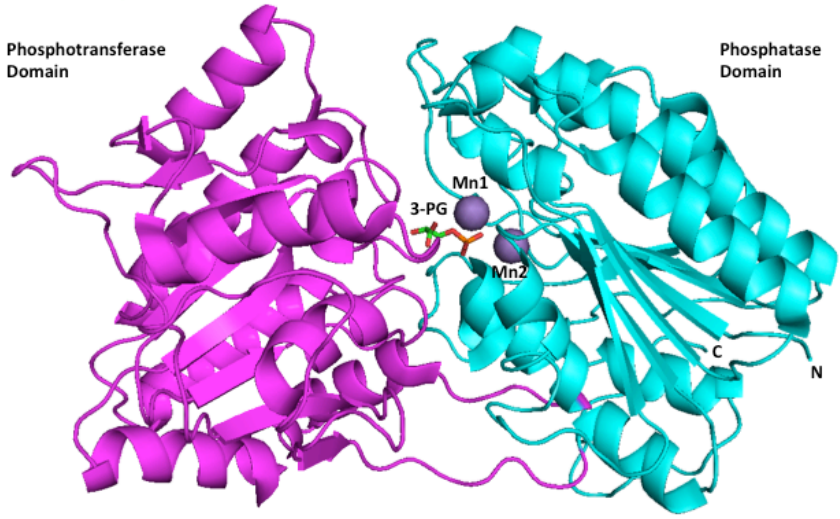

Figure 1-3. General structure of iPGM enzyme. (PDB: 1EJJ) Phosphotransferase domain and phosphatase domain are colored in purple and cyan respectively along with 3-PG substrate and two Manganese ions in the active site.

Wide ranges of organisms possess iPGM, including bacteria, nematodes and plants (Figure 1-5). The molecular and biochemical characterization of iPGMs demonstrate that their catalytic properties are highly conserved; with active site contains 12 amino acid residues, a catalytic reactive serine and divalent metal ions of manganese, magnesium or cobalt.[47] 12 Amino acid residues are involved in catalysis or interacting with metal ions.[48] Divalent metal ions are also crucial elements for iPGMs activity, since these ions participate the catalysis and maintain the structural integrity.[29]

In contrast, dPGM, a PGM isozyme is composed of ~250 amino acids and catalyzes the intermolecular transfer of the phosphate group between the mono-phosphoglycerate and the cofactor (2,3-diphosphoglycerate) by forming an intermediate of phosphohistidine (Figure 1-2).[49,50] Furthermore, the active form of dPGM has no requirement of metal ions. Vertebrates or mammals including human are known to only possess dPGM. dPGM and iPGM have no sequence and structural similarity as well as catalytic mechanism identity.[44]

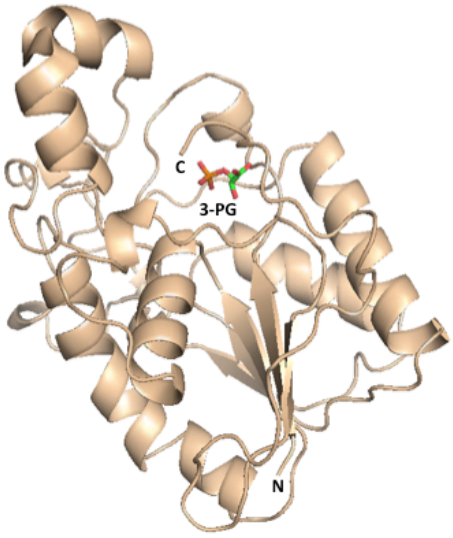

Figure 1-4. Overall structure of dPGM with 3-PG substrate in active site. (PDB: 1QBHF)

The distribution of two PGM enzyme classes was summarized in Figure 1-5. Generally, iPGMs mainly exist in higher plants, nematodes, archaea and many bacteria, while vertebrates, yeasts, and many other bacteria possess only dPGM. A little number of bacteria, like *Escherichia coli* and certain archaea and protozoa, has both forms of PGM. Therefore iPGM is considered as a promising anti-microbial drug target; iPGM inhibitor would effectively inhibit wide range of iPGM orthologs, due to their similarities in structure and catalytic mechanism.[39]

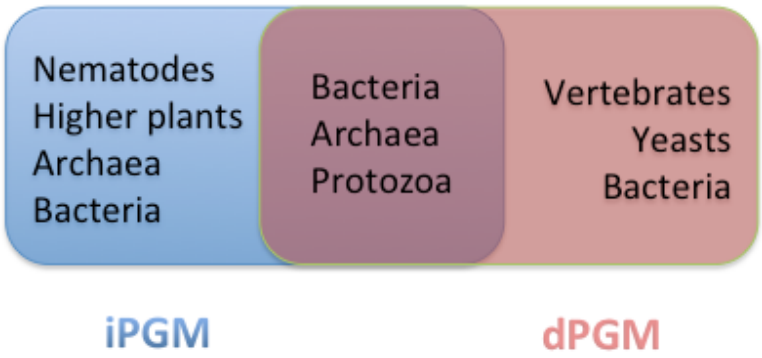

Figure 1-5. The distribution of iPGM and dPGM in organisms. Organisms shown in blue box and red box contain iPGM and dPGM enzyme respectively.

1.4 Anti-parasite drug discovery against iPGM and the RaPID system

iPGM has been proved to be an important enzyme for the development and survival of parasitic nematodes. As previously described, the down regulation of iPGM gene transcript leads to sluggish movement and embryonic lethality in nematodes. On the other hand, iPGMs are absent from parasite host animals. Thus, iPGM has been a promising target for anti-parasite therapeutics.[51,52]

Target-based screening methods have been prevalence and productive approaches to generate drug-like compounds by screening molecular libraries containing natural products or synthetic compounds.[53] Among the methods, High Throughput Screening (HTS) is a representative screening strategy for discovering novel active molecules against specific targets. Recently, iPGM from *B. malayi* and *C. elegans* have been cloned and characterized and readily for HTS. In the hope of obtaining iPGM inhibitors, an attempt to obtain small molecule inhibitors against *B. malayi* and *C. elegans* iPGM were performed. Nevertheless, compounds isolated from this attempt do not exhibit desired inhibitory activity, the IC_{50} value of selected molecules are only μM level.[31,45] Since, the substrates of iPGM enzyme (3-PG and 2-PG) are highly polar molecules and the active site of iPGM is hydrophobic which limit the access of small compounds during HTS, thus they considered iPGM as a target with low druggability. Therefore traditional drug discovery approaches with small molecules did not derive potent inhibitors against iPGM, no potent iPGM inhibitors have been reported to date.

Comparing to small molecular compounds which do not have sufficient interaction surface, peptides have attracted increasing attention as drug resources, and display advantages such as extended binding interface, high target affinity and specificity, derived from the property of various amino acid sidechains.[54,55] Furthermore, peptides possessing cyclic structure and non-canonical amino acids have been discovered and showed diverse advantages as therapeutics. Investigations have demonstrated that cyclic structure is a favored feature in many therapeutic agents.[56] Since backbone cyclization keeps the peptide in a constrained state and holds the sidechain of amino acid in proper orientation to interact with targets. Non-canonical amino acids like

D-amino acids, *N*-methyl amino acids have also been discovered in natural peptide product which showed potent bioactivity. These features would improve peptide drug-like properties such as membrane permeability or proteases resistant.

The Random non-standard Peptide Integrated Discovery (RaPID) system is an advanced *in vitro* peptide screening technology developed in our lab.[57,58] This approach enables the rapid selection of high affinity target-binders from a genetic code reprogrammed peptide library containing trillions of unique macrocyclic peptides. The RaPID system is comprised of mRNA display technology and the Flexible *in vitro* translation (FIT) system.[59-61] The FIT system is an optimized and improved custom-made reconstituted cell-free in vitro translation system integrated with Flexizymes. Flexizymes are *de novo* tRNA acylation ribozymes developed in our laboratory and have the ability of charging various amino acids onto desired tRNAs. The FIT system enables us to prepare non-canonical amino acids charged tRNA and introduce various non-standard features including thioether-bond, D-amino acid, N-methyl amino acids with non-canonical side chain that would mimic natural products and improve drug-like property of peptides (Figure 1-6).

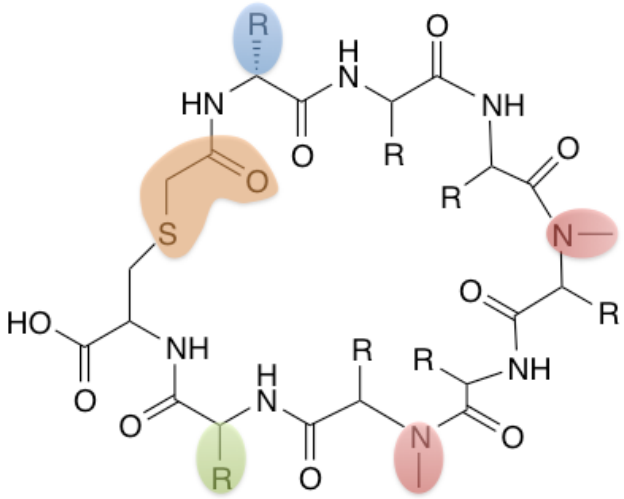

Figure 1-6. General structural features in macrocyclic peptide generated by the RaPID system. Thioether bond (in orange), D-amino acid (in blue), N-methylation (in red) and non-canonical sidechains (in green) such as warhead are showed.

The RaPID system has lead to discovery of bioactive macrocyclic peptides targeting various proteins and protein-protein interactions (Table1-2).[62-64] Novel peptide inhibitors were identified against Akt2 (serine/threonine-specific protein kinase), Sirt2 (NAD-dependent deacetylase) and E6AP (ubiquitin ligase). Peptide inhibitors were discovered toward MATE (multi antimicrobial extrusion), the crystal structure of peptide-protein complex revealed the binding and inhibition mode of macrocyclic peptides. Recently, macrocyclic peptides binding to cMET (receptor tyrosine kinase) were also discovered and exhibit agonist activity after dimerization. Based on these successful drug discovery campaigns, we consider macrocyclic peptides as promising compound class in therapeutic discovery and the RaPID system as a promising tool for developing novel peptide agent against various therapeutic targets. Therefore, the RaPID system was employed to develop macrocyclic inhibitors against iPGMs in this study.

Table 1-2. The bioactive macrocyclic peptides discovered by using the RaPID system against various target protein.

Macrocyclic peptides	Target protein	Class	Affinity (K_D)	Activity	Features
Pakti-L1	Akt2	Enzyme	—	Inhibition (IC_{50}=110nM)	Isoform-selectivity
S2iL8, S2iD7	Sirt2	Enzyme	3.7-3.8 nM	Inhibition (IC_{50}=3.2-3.7 nM)	Isoform-selectivity, Warhead
CM_{11}-1	E6AP	Enzyme	0.6 nM	Inhibition	N-methyl peptide
MaD5, MaD3S, MaL6	pfMATE	Transporter	—	Inhibition	Lariat-like peptide
aML5, aMD4, aMD5	cMET	-	2-19 nM	Agonist	Dimeric peptide

1.5 References

1 Ghedin, E. *et al.* Draft genome of the filarial nematode parasite Brugia malayi. *Science* **317**, 1756-1760 (2007).

2 Burns, A. R. *et al.* Caenorhabditis elegans is a useful model for anthelmintic discovery. *Nature communications* **6** (2015).

3 WHO. Global programme to eliminate lymphatic filariasis: progress report on mass drug adminstration. *Weekly epidemiological record*. Vol. 86, 35 377-388 (2011).

4 Whitworth, J. A. G. & Hewitt, K. Filariasis. *Medicine* **33**, 61-64 (2005).

5 Taylor, M. J. & Hoerauf, A. Wolbachia bacteria of filarial nematodes. *Parasitology today* **15**, 437-442 (1999).

6 Donahoe, J. M. R. Experimental infection of cats with Dirofilaria immitis. *The Journal of parasitology*, 599-605 (1975).

7 Lustigman, S. *et al.* A research agenda for helminth diseases of humans: the problem of helminthiases. *PLoS Negl Trop Dis* **6**, e1582 (2012).

8 McCall, J. W., Genchi, C., Kramer, L. H., Guerrero, J. & Venco, L. Heartworm disease in animals and humans. *Advances in parasitology* **66**, 193-285 (2008).

9 Taylor, M. J., Hoerauf, A. & Bockarie, M. Lymphatic filariasis and onchocerciasis. *The Lancet* **376**, 1175-1185 (2010).

10 Li, Z., Galvin, B. D., Raverdy, S. & Carlow, C. K. S. Identification and characterization of the cofactor-independent phosphoglycerate mutases of Dirofilaria immitis and its Wolbachia endosymbiont. *Veterinary parasitology* **176**, 350-356 (2011).

11 Gyapong, J. O., Kumaraswami, V., Biswas, G. & Ottesen, E. A. Treatment strategies underpinning the global programme to eliminate lymphatic filariasis. *Expert opinion on pharmacotherapy* **6**, 179-200 (2005).

12 McGarry, H. F., Plant, L. D. & Taylor, M. J. Diethylcarbamazine activity against Brugia malayi microfilariae is dependent on inducible nitric-oxide synthase and the cyclooxygenase pathway. *Filaria journal* **4**, 1 (2005).

13 Basanez, M.-G. *et al.* Effect of single-dose ivermectin on Onchocerca volvulus: a systematic review and meta-analysis. *The Lancet infectious*

diseases **8**, 310-322 (2008).

14 Wolstenholme, A. J. & Rogers, A. T. Glutamate-gated chloride channels and the mode of action of the avermectin/milbemycin anthelmintics. *Parasitology* **131**, S85-S95 (2005).

15 Ottesen, E. A., Ismail, M. M. & Horton, J. The role of albendazole in programmes to eliminate lymphatic filariasis. *Parasitology Today* **15**, 382-386 (1999).

16 Hoerauf, A., Pfarr, K., Mand, S., Debrah, A. Y. & Specht, S. Filariasis in Africa—treatment challenges and prospects. *Clinical Microbiology and Infection* **17**, 977-985 (2011).

17 Ismail, M. M. *et al.* Efficacy of single dose combinations of albendazole, ivermectin and diethylcarbamazine for the treatment of bancroftian filariasis. *Transactions of the Royal Society of Tropical Medicine and Hygiene* **92**, 94-97 (1998).

18 Sharma, D. C. New goals set for filariasis elimination in India. *The Lancet Infectious Diseases* **2**, 389 (2002).

19 Fischer, P., Supali, T. & Maizels, R. M. Lymphatic filariasis and Brugia timori: prospects for elimination. *Trends in parasitology* **20**, 351-355 (2004).

20 Mohammed, K. A., Molyneux, D. H., Albonico, M. & Rio, F. Progress towards eliminating lymphatic filariasis in Zanzibar: a model programme. *Trends in parasitology* **22**, 340-344 (2006).

21 Philipp, M., Davis, T. B., Storey, N. & Carlow, C. K. S. Immunity in filariasis: perspectives for vaccine development. *Annual Reviews in Microbiology* **42**, 685-716 (1988).

22 Gilleard, J. S. The use of Caenorhabditis elegans in parasitic nematode research. *Parasitology* **128**, S49-S70 (2004).

23 Bürglin, T. R., Lobos, E. & Blaxter, M. L. Caenorhabditis elegans as a model for parasitic nematodes. *International journal for parasitology* **28**, 395-411 (1998).

24 Geary, T. G. & Thompson, D. P. Caenorhabditis elegans: how good a model for veterinary parasites? *Veterinary Parasitology* **101**, 371-386 (2001).

25 Foster, J. M., Zhang, Y., Kumar, S. & Carlow, C. K. S. Mining nematode

genome data for novel drug targets. *Trends in parasitology* **21**, 101-104 (2005).

26 Foster, J. M. *et al.* The Wolbachia endosymbiont of Brugia malayi has an active phosphoglycerate mutase: a candidate target for anti-filarial therapies. *Parasitology research* **104**, 1047-1052 (2009).

27 Kumar, S. *et al.* Mining predicted essential genes of Brugia malayi for nematode drug targets. *PloS one* **2**, e1189 (2007).

28 Blaxter, M., Daub, J., Guiliano, D., Parkinson, J. & Whitton, C. The Brugia malayi genome project: expressed sequence tags and gene discovery. *Transactions of the Royal Society of Tropical Medicine and Hygiene* **96**, 7-17 (2002).

29 Raverdy, S., Zhang, Y., Foster, J. & Carlow, C. K. S. Molecular and biochemical characterization of nematode cofactor independent phosphoglycerate mutases. *Molecular and biochemical parasitology* **156**, 210-216 (2007).

30 Chander, M., Setlow, P., Lamani, E. & Jedrzejas, M. J. Structural studies on a 2, 3-diphosphoglycerate independent phosphoglycerate mutase from Bacillus stearothermophilus. *Journal of structural biology* **126**, 156-165 (1999).

31 Jedrzejas, M. J., Chander, M., Setlow, P. & Krishnasamy, G. Mechanism of Catalysis of the Cofactor-independent Phosphoglycerate Mutase from Bacillus stearothermophilus Crystal structure of the complex with 2-phosphoglycerate. *Journal of Biological Chemistry* **275**, 23146-23153 (2000).

32 Aboobaker, A. A. & Blaxter, M. L. Use of RNA interference to investigate gene function in the human filarial nematode parasite Brugia malayi. *Molecular and biochemical parasitology* **129**, 41-51 (2003).

33 Singh, P. K., Kushwaha, S., Mohd, S., Pathak, M. & Misra-Bhattacharya, S. In vitro gene silencing of independent phosphoglycerate mutase (iPGM) in the filarial parasite Brugia malayi. *Infectious Diseases of Poverty* **2**, 1 (2013).

34 Chevalier, N., Rigden, D. J., Van Roy, J., Opperdoes, F. R. & Michels, P. A. M. Trypanosoma brucei contains a 2, 3 - bisphosphoglycerate independent

phosphoglycerate mutase. *European Journal of Biochemistry* **267**, 1464-1472 (2000).

35 Guerra, D. G., Vertommen, D., Fothergill‐Gilmore, L. A., Opperdoes, F. R. & Michels, P. A. M. Characterization of the cofactor‐independent phosphoglycerate mutase from Leishmania mexicana mexicana. *European Journal of Biochemistry* **271**, 1798-1810 (2004).

36 Besteiro, S., Barrett, M. P., Rivière, L. & Bringaud, F. Energy generation in insect stages of Trypanosoma brucei: metabolism in flux. *Trends in parasitology* **21**, 185-191 (2005).

37 Djikeng, A. *et al.* Cofactor-independent phosphoglycerate mutase is an essential gene in procyclic form Trypanosoma brucei. *Parasitology research* **100**, 887-892 (2007).

38 Foster, J. M. *et al.* Evolution of bacterial phosphoglycerate mutases: non-homologous isofunctional enzymes undergoing gene losses, gains and lateral transfers. *PloS one* **5**, e13576 (2010).

39 Zhang, Y., Foster, J. M., Kumar, S., Fougere, M. & Carlow, C. K. S. Cofactor-independent phosphoglycerate mutase has an essential role in Caenorhabditis elegans and is conserved in parasitic nematodes. *Journal of Biological Chemistry* **279**, 37185-37190 (2004).

40 O'Reilly, L. P., Luke, C. J., Perlmutter, D. H., Silverman, G. A. & Pak, S. C. C. elegans in high-throughput drug discovery. *Advanced drug delivery reviews* **69**, 247-253 (2014).

41 Jedrzejas, M. J. Structure, function, and evolution of phosphoglycerate mutases: comparison with fructose-2, 6-bisphosphatase, acid phosphatase, and alkaline phosphatase. *Progress in biophysics and molecular biology* **73**, 263-287 (2000).

42 Fothergill-Gilmore, L. A. & Watson, H. C. The phosphoglycerate mutases. *Adv Enzymol Relat Areas Mol Biol* **62**, 227-313 (1989).

43 Graña, X. *et al.* 2, 3-Bisphosphoglycerate-independent phosphoglycerate mutase is conserved among different phylogenic kingdoms. *Comparative Biochemistry and Physiology Part B: Biochemistry and Molecular Biology* **112**, 287-293 (1995).

44 Rigden, D. J., Mello, L. V., Setlow, P. & Jedrzejas, M. J. Structure and

mechanism of action of a cofactor-dependent phosphoglycerate mutase homolog from Bacillus stearothermophilus with broad specificity phosphatase activity. *Journal of molecular biology* **315**, 1129-1143 (2002).

45 Jedrzejas, M. J., Chander, M., Setlow, P. & Krishnasamy, G. Structure and mechanism of action of a novel phosphoglycerate mutase from Bacillus stearothermophilus. *The EMBO journal* **19**, 1419-1431 (2000).

46 Nukui, M. *et al.* Structure and molecular mechanism of Bacillus anthracis cofactor-independent phosphoglycerate mutase: a crucial enzyme for spores and growing cells of Bacillus species. *Biophysical journal* **92**, 977-988 (2007).

47 Jedrzejas, M. J. & Setlow, P. Comparison of the binuclear metalloenzymes diphosphoglycerate-independent phosphoglycerate mutase and alkaline phosphatase: their mechanism of catalysis via a phosphoserine intermediate. *Chemical reviews* **101**, 607-618 (2001).

48 Galperin, M. Y., Koonin, E. V. & Bairoch, A. A superfamily of metalloenzymes unifies phosphopentomutase and cofactor‐independent phosphoglycerate mutase with alkaline phosphatases and sulfatases. *Protein Science* **7**, 1829-1835 (1998).

49 Bond, C. S., White, M. F. & Hunter, W. N. Mechanistic implications for Escherichia coli cofactor-dependent phosphoglycerate mutase based on the high-resolution crystal structure of a vanadate complex. *Journal of molecular biology* **316**, 1071-1081 (2002).

50 Fraser, H. I., Kvaratskhelia, M. & White, M. F. The two analogous phosphoglycerate mutases of Escherichia coli. *FEBS letters* **455**, 344-348 (1999).

51 Brown, D. & Superti-Furga, G. Rediscovering the sweet spot in drug discovery. *Drug discovery today* **8**, 1067-1077 (2003).

52 L Hopkins, A. *et al.* Rapid analysis of pharmacology for infectious diseases. *Current topics in medicinal chemistry* **11**, 1292-1300 (2011).

53 Nwaka, S. & Hudson, A. Innovative lead discovery strategies for tropical diseases. *Nature Reviews Drug Discovery* **5**, 941-955 (2006).

54 Craik, D. J., Fairlie, D. P., Liras, S. & Price, D. The future of peptide‐based

drugs. *Chemical biology & drug design* **81**, 136-147 (2013).

55 McGregor, D. P. Discovering and improving novel peptide therapeutics. *Current opinion in pharmacology* **8**, 616-619 (2008).

56 Driggers, E. M., Hale, S. P., Lee, J. & Terrett, N. K. The exploration of macrocycles for drug discovery—an underexploited structural class. *Nature Reviews Drug Discovery* **7**, 608-624 (2008).

57 Hipolito, C. J. & Suga, H. Ribosomal production and in vitro selection of natural product-like peptidomimetics: the FIT and RaPID systems. *Current opinion in chemical biology* **16**, 196-203 (2012).

58 Passioura, T. & Suga, H. Flexizyme‐Mediated Genetic Reprogramming As a Tool for Noncanonical Peptide Synthesis and Drug Discovery. *Chemistry–A European Journal* **19**, 6530-6536 (2013).

59 Goto, Y., Katoh, T. & Suga, H. Flexizymes for genetic code reprogramming. *Nature protocols* **6**, 779-790 (2011).

60 Murakami, H., Ohta, A., Ashigai, H. & Suga, H. A highly flexible tRNA acylation method for non-natural polypeptide synthesis. *Nature Methods* **3** (2006).

61 Ohuchi, M., Murakami, H. & Suga, H. The flexizyme system: a highly flexible tRNA aminoacylation tool for the translation apparatus. *Current opinion in chemical biology* **11**, 537-542 (2007).

62 Yamagishi, Y. *et al.* Natural product-like macrocyclic N-methyl-peptide inhibitors against a ubiquitin ligase uncovered from a ribosome-expressed de novo library. *Chemistry & biology* **18**, 1562-1570 (2011).

63 Hayashi, Y., Morimoto, J. & Suga, H. In vitro selection of anti-Akt2 thioether-macrocyclic peptides leading to isoform-selective inhibitors. *ACS chemical biology* **7**, 607-613 (2012).

64 Ito, K. *et al.* Artificial human Met agonists based on macrocycle scaffolds. *Nature communications* **6** (2015).

Chapter 2

Discovery of inhibitory macrocyclic peptides against *B. malayi* iPGM

2.1 Introduction

Cofactor independent phosphoglycerate mutase (iPGM) is an essential metabolic enzyme for survival and development of many microbial organisms and has been identified as a promising target for development of anti-parasite drugs.[1] The genome and RNAi studies have confirmed iPGM as an essential enzyme for *Brugia malayi*, which is a parasitic nematode causing Lymphatic Filariasis disease.[2] Therefore *B. malayi* iPGM has been considered as a potential drug target for Lymphatic Filariasis disease treatment. However no potent *B. malayi* iPGM inhibitors have been reported to date.[3] A recent attempt of HTS studies on iPGMs did not discover potent inhibitors from small molecule libraries.[4] Thus, Alternative drug classes are needed and could be resources for iPGM inhibitors discovery.

In this chapter, I performed *in vitro* affinity selection to discover *B. malayi* iPGM binding macrocyclic peptides by using the RaPID system. The binding and inhibitory activity of selected peptides would be evaluated to identify iPGM inhibitors.

2.2 Results and discussions

2.2.1 Discovery of *B. malayi* iPGM-binding macrocyclic peptides by using the RaPID system

An *in vitro* affinity selection was performed by the means of the RaPID system. For this selection, an mRNA library encoding trillions of macrocyclic peptides was prepared firstly. Then, the mRNAs were ligated with a Puromycin linker and translated, which resulted in mRNA-peptide conjugates. These resultant peptides have an initiator amino acid of *N*-chloroacetyl-D-Tyrosine (ClAc-tyrosine) followed by random amino acid region containing 4 to 12 amino acids and an C-terminal cysteine followed by a linker region of GSGSGS (G=glycine, S=serine). After translation, a thioether bond formed spontaneously between the chloroacetyl group of N-terminal ClAc-tyrosine and the sulfhydryl group of C-terminal cysteine to generate macrocyclic structure. This prepared peptide library was then subject to the selection procedure (Figure 2-1).

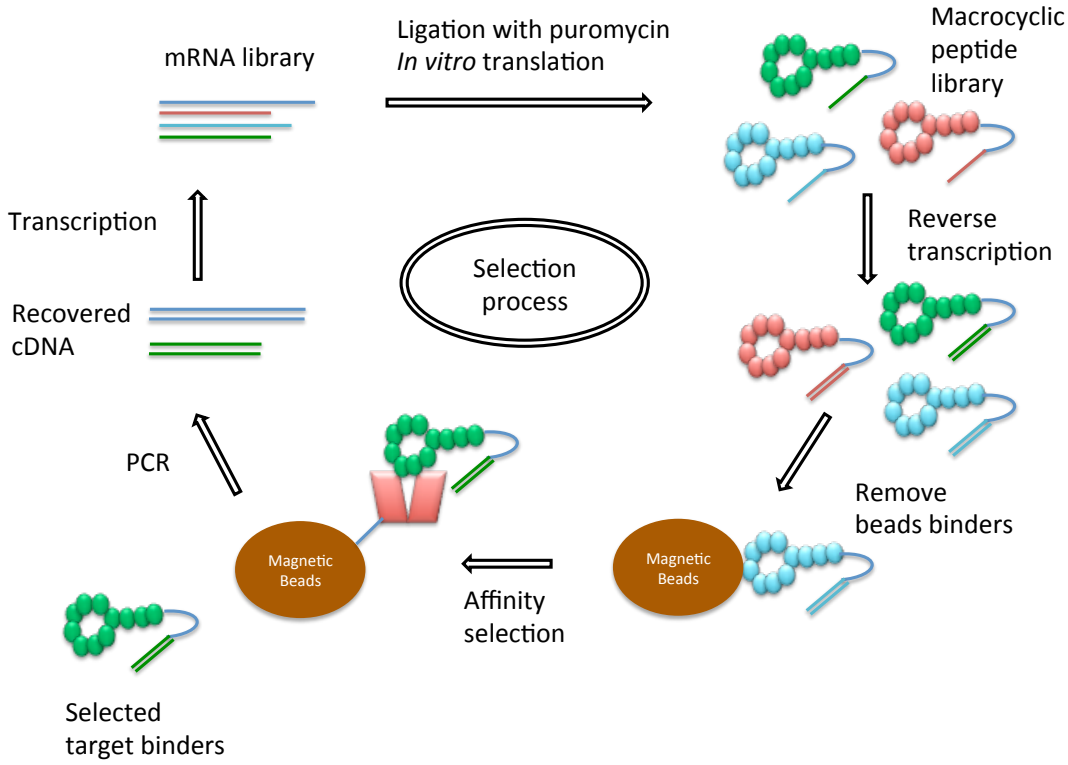

Figure 2-1. Schematic presentation and work flow of target binding macrocyclic peptides selection using the RaPID system.

A His_{10}-tagged *B. malayi* iPGM was used as target protein in this study and immobilized to magnetic beads (His-tag Isolation & Pull-down Dynabeads). The prepared peptide library was incubated with only magnetic beads to remove undesired beads binding peptides. The remained peptide library was then applied to *B. malayi* iPGM immobilized magnetic beads to isolated specific peptides bind to *B. malayi* iPGM. The amount of beads-binding peptides and *B. malayi* iPGM-binding peptides were monitored by RT-PCR of the quantity of peptide-mRNA fusions. cDNAs were amplified and transcribed as mRNA library for the next round of selection (Figure 2-1).

The enrichment of *B. malayi* iPGM binding peptides was observed after the fifth round selection and The cDNA recovery rate of *B. malayi* iPGM binders reached 7.4% at the sixth round, while the beads-binding peptides was suppressed significantly (Figure 2-2). This observation indicated that specific *B. malayi* iPGM binding peptides were being enriched.

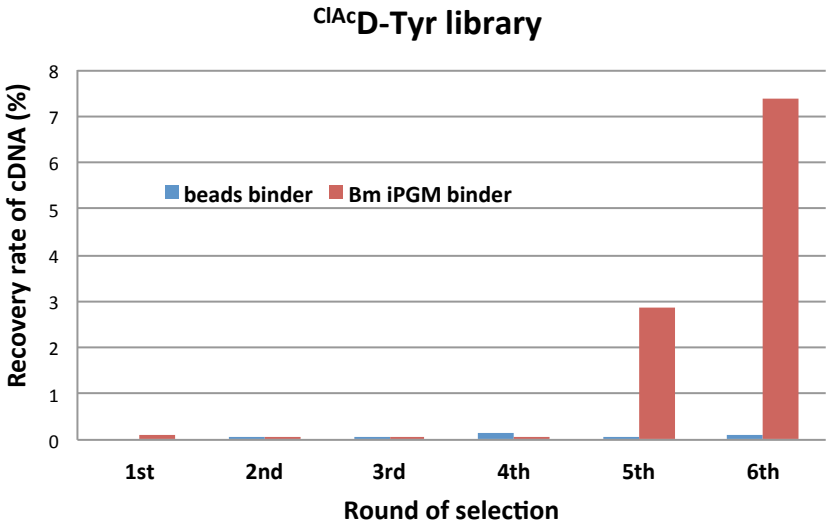

Figure 2-2. The enrichment of *B. malayi* iPGM binding peptides is represented by the recovery rate of cDNA amount in each round of selection. Red bars and blue bars represented the quantity of cDNA from magnetic beads and *B. malayi* immobilized beads, respectively.

2.2.2 Macrocyclic peptides identified by *in vitro* affinity selection

The recovered cDNAs from fourth, fifth and sixth round of selection were cloned by TA cloning technique and sequenced to obtain the sequence information. By analyzing of 23 clones, 12 macrocyclic peptides were determined as candidate *B. malayi* iPGM binders (Table 2-1). A conserved WPN (TrpProAsn) sequence was observed in the random region of 5 peptides. 2 peptides contained WL (TrpLeu) sequence with different length. The last 5 peptides appeared once with no sequence similarity.

Table 2-1. The peptide sequences derived from recovered cDNA

Sequence	Frequency
LDWPNCSTC	7/23
LEWPNCNTC	4/23
AVWPNCRTC	3/23
PEWPNCSTC	1/23
SWPNAPEIWKCC	1/23
DLRTPWLKRHAC	1/23
QNRSIWLYGCC	1/23
HHAQRYCKPC	1/23
RHYVCKKPSGHC	1/23
HKLSYMVCVC	1/23
LHPLFMHDRDRTC	1/23
LYCLVCWSWCC	1/23

Seven peptides (named as Bm-1~Bm-7), which are containing conserved WPN or WL sequence, were chosen to further confirm their binding ability against *B. malayi* iPGM. As in affinity selection, these peptides were prepared firstly and then incubated with magnetic beads and *B. malayi* iPGM immobilized magnetic beads respectively. The recovery quantity of each peptide was determined (Figure 2-3). All the seven peptides selectively bound to *B. malayi* iPGM (immobilized on magnetic beads) and exhibit 2~185 fold selectivity against only magnetic beads.

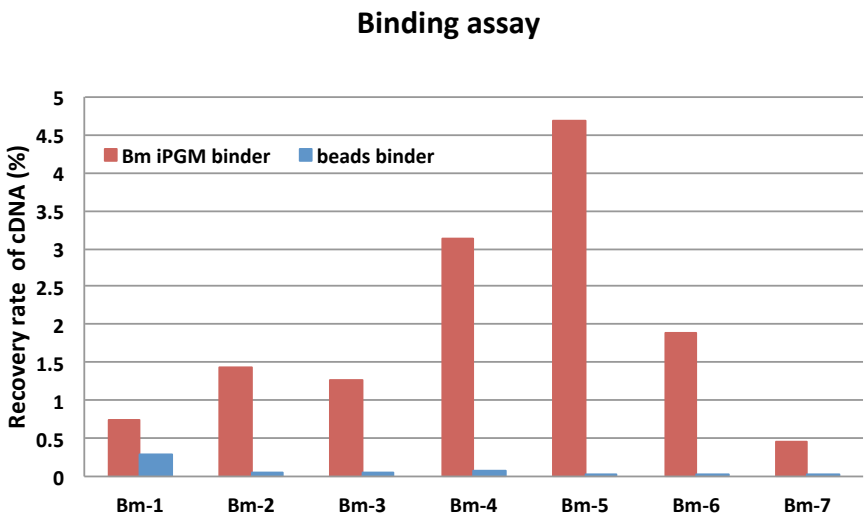

Figure 2-3. Evaluation of macrocyclic peptides binding activity. Bm-1 to Bm-7 can selectively bind to *B. malayi* iPGM immobilized magnetic beads.

Among the selected macrocyclic peptides, Bm-1 to Bm-3 are macrocyclic peptides with a short tail peptide. Bm-4 to Bm-7 are lariat-like peptides having cyclic head of seven amino acids and tail peptide with four residues. Interestingly, two cysteine residues appeared in this peptide family. One cysteine locates at 7th amino acid position and another one locates at the C-terminus of the peptide. This distribution of cysteine residue resulted in cyclized peptide with a lariat structure. These macrocyclic peptides are chemically synthesized and purified by reverse phase HPLC for further inhibitory activity assay.

Table 2-2. The sequence information of *B. malayi* iPGM binding peptides

Peptide ID	Sequence	Ring size/Tail length
Bm-1	Ac-DYSWPNAPEIWKCCG (S)	12/2
Bm-2	Ac-DYDLRTPWLKRHACG (S)	13/1
Bm-3	Ac-DYQNRSIWLYGCG (S)	11/1
Bm-4	Ac-DYLEWPNCNTCG (S)	7/4
Bm-5	Ac-DYLDWPNCSTCG (S)	7/4
Bm-6	Ac-DYPEWPNCSTCG (S)	7/4
Bm-7	Ac-DYAVWPNCRTCG (S)	7/4

2.2.3 Evaluation of inhibitory activity of selected peptides

Inhibitory activity of identified macrocyclic peptides was evaluated by an enzyme-coupled assay against PGMs from seven organisms, including five iPGMs orthologs from *B. malayi*, *C. elegans*, *O. volvulus*, *D. immitis* and *E. coli* and two dPGM isozymes from *E. coli* and *H. sapiens*. A kinetic and endpoint assay based on 1536-well plate was used to detect the conversion of 3-PG to 2-PG catalyzed by PGM enzymes. The 2-PG product was converted to pyruvate and lactate plus an ATP via enolase and pyruvate kinase, respectively. The ATP product and a luciferin are catalyzed by firefly luciferase to generate light production. The light intensity that reflects the activity of PGM enzyme will be detected and quantified. The activity of PGMs was determined indirectly through this way.

The inhibitory activities of candidate peptides were determined and most peptides exhibited inhibitory activity except Bm-2 (Table 2-3). Active peptides can not only inhibit target protein of *B. malayi* iPGM with pIC_{50} values of 5.56-6.26 (IC_{50} = 0.55-2.7 μM), but also show inhibitory activity toward four iPGM orthologs from parasite and bacteria. On the other hand, active macrocyclic peptides showed inhibitory selectivity against dPGM enzymes, isozyme of iPGM in human.

Table 2-3. The inhibitory activity of selected macrocyclic peptides against target enzyme *B. malayi* iPGM and four iPGM orthologs from *C. elegans*, *O. volvulus*, *D. immitis* and *E. coli*, two PGM isozyme from *E. coli* and *H. sapiens* .

Peptide ID	Sequence	pIC_{50}						
		B.malayi iPGM	C. elegans iPGM	O. volvulus iPGM	D. immitis iPGM	E. coli iPGM	E. coli dPGM	H. sapiens dPGM
Bm-1	Ac-DYSWPNAPEIWKCCG (S–S)	5.89	5.30	5.88	5.99	5.31	NA	NA
Bm-2	Ac-DYDLRTPWLKRHACG (S–S)	NA	NA	NA	NA	NA	NA	NA
Bm-3	Ac-DYQNRSIWLYGCG (S–S)	5.56	5.05	5.88	5.99	5.31	NA	NA
Bm-4	Ac-DYLEWPNCNTCG (S–S)	6.26	5.61	6.10	6.21	5.56	NA	NA
Bm-5	Ac-DYLDWPNCSTCG (S–S)	6.16	5.60	5.99	6.10	5.54	NA	NA
Bm-6	Ac-DYPEWPNCSTCG (S–S)	6.16	5.58	6.08	6.26	5.55	NA	NA
Bm-7	Ac-DYAVWPNCRTCG (S–S)	5.28	5.13	5.37	5.42	5.12	NA	NA

pIC_{50}= -log IC_{50}, ex. pIC_{50}=9 equal $IC_{50}=10^{-9}$ M. NA = No appreciable inhibitory activity at highest concentration tested.

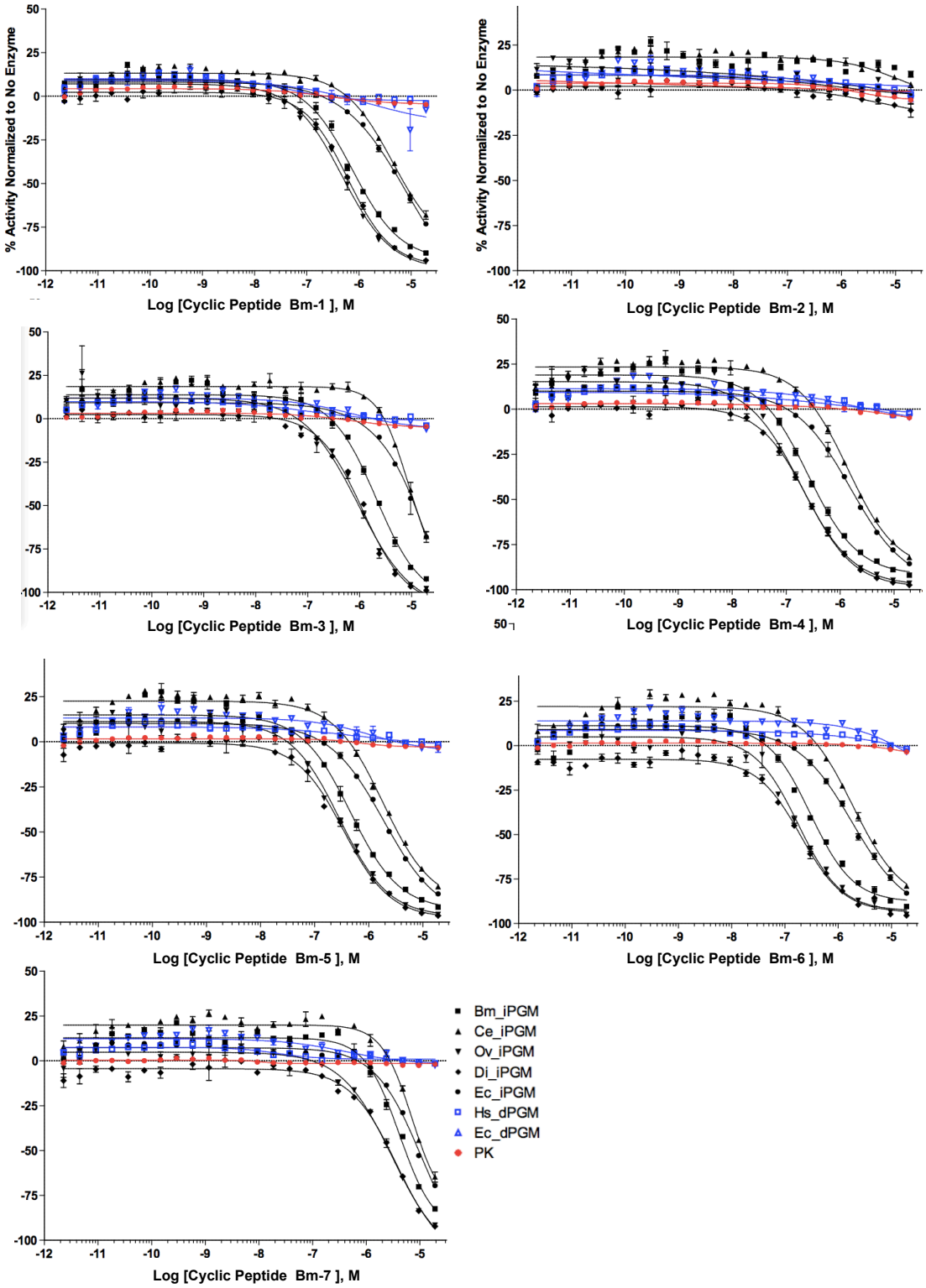

Figure 2-4. IC_{50} concentration-response curves for characterization of Bm-1 to Bm-7 on the iPGM orthologs and dPGM isozymes using the enzyme coupled bioluminescent assay.

2.2.4 Importance of tail residues for inhibitory activity

Peptide Bm-4 with lariat-like structure was the most potent inhibitor among the active peptides. In order to examine the respective function of the cyclic head structure and linear tail peptide in Bm-4, a series of C-terminal truncated Bm-4 analogs was prepared and evaluated for inhibitory activity (Table 2-4). The results displayed that the tail peptide contributes to the inhibitory activity of Bm-4, especially the C-terminus cys10. Once this cys10 residue was deleted, the peptide lost inhibitory ability against all iPGM orthologs. On the other hand, another Bm-4 analog was also prepared in which the cys10 residue was substituted by a serine residue and tested for inhibitory activity. The replacement of cysteine by serine resulted in significant negative effect on inhibitory activity. The inhibitory activity totally lost against all iPGMs. These observations demonstrated that the C-terminal cysteine residue is important for the inhibitory activity in Bm-4.

Table 2-4. The inhibitory activity of truncation and Ser substitution analogs of Bm-4 against target enzyme *B. malayi* iPGM and four iPGM orthologs from *C. elegans*, *O. volvulus*, *D. immitis* and *E. coli*, two PGM isozyme from *E. coli* and *H. sapiens* .

Peptide ID	Sequence	pIC_{50}						
		B.malayi iPGM	*C. elegans* iPGM	*O. volvulus* iPGM	*D. immitis* iPGM	*E. coli* iPGM	*E. Coli* dPGM	*H. sapiens* dPGM
Bm-4	Ac-D  YLEWPNCNTCG	6.26	5.61	6.10	6.21	5.56	NA	NA
Bm-4S	Ac-D  YLEWPNCNTS	NA	NA	NA	NA	NA	NA	NA
Bm-4-1	Ac-D 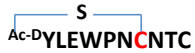 YLEWPNCNTC	6.31	5.61	6.14	6.28	5.58	NA	NA
Bm-4-2	Ac-D  YLEWPNCNT	NA	NA	NA	NA	NA	NA	NA
Bm-4-3	Ac-D  YLEWPNCN	NA	NA	NA	NA	NA	NA	NA
Bm-4-4	Ac-D  YLEWPNC	NA	NA	NA	NA	NA	NA	NA

pIC_{50}= -log IC_{50}, ex. pIC_{50}=9 equal $IC_{50}=10^{-9}$ M. NA = No appreciable inhibitory activity at highest concentration tested,

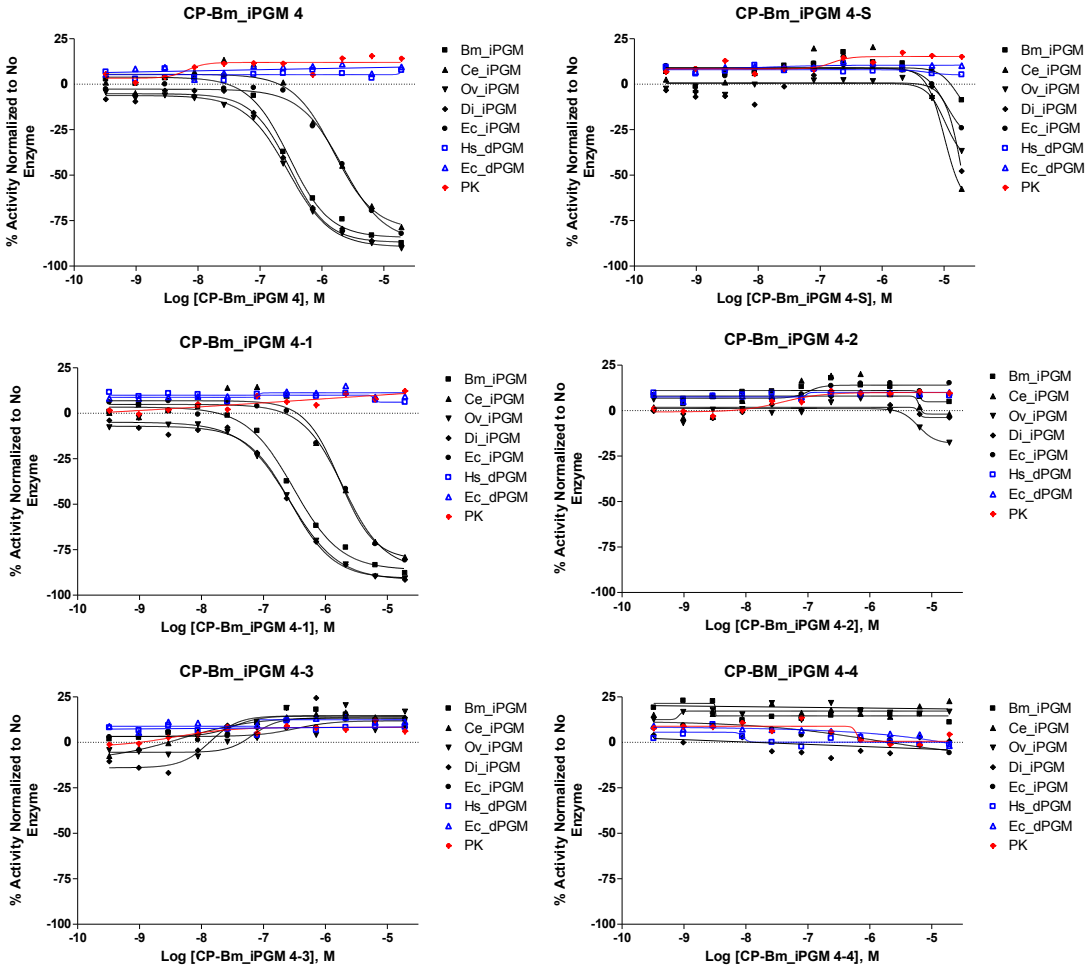

Figure 2-5. IC_{50} concentration-response curves for characterization of Bm-4-1 to Bm-4-4 and Bm-4S on the iPGM orthologs and dPGM isozymes using the enzyme coupled bioluminescent assay.

2.3 Conclusion

In this study, Seven *B. malayi* iPGM binding macrocyclic peptides were successfully isolated via *in vitro* affinity selection by using the RaPID system. Six peptides showed inhibitory activity against *B. malayi* iPGM and four iPGM orthologs and isozyme selectivity toward dPGM. Among selected peptides, Bm-4 was an potent *B. malayi* iPGM inhibitor (pIC_{50} = 6.26, IC_{50} = 0.55 μM) and exhibited broad-spectrum inhibitory activity against iPGM orthologs. To our knowledge, it is the first time to discover peptide iPGM inhibitors. Furthermore, the function of tail peptide in Bm-4 was studied by truncation modification study. The results revealed that the tail peptide is crucial for inhibitory activity. Cysteine residue at the C-terminal was proved to be a crucial residue for inhibitory and broad-spectrum activity.

It is remarkable that even though iPGM was considered as an "undruggable" protein, macrocyclic peptide inhibitors were identified and exhibited inhibitory activity against *B. malayi* iPGM and broadly inhibit iPGM orthologs in this study. Macrocyclic peptides were proved as promising compound class for the development of anti-parasite therapeutics. The identification of macrocyclic peptide inhibitors provides insight on drug discovery against otherwise undruggable targets. Therefore I extensively attempt to discover novel potent iPGM inhibitors by means of the RaPID system in the next chapter.

2.4 Materials and experimental section

2.4.1 General

All Chemical reagents were purchased commercially from Watanabe Chemical Industry, Nacalai Tasque, Tokyo chemical industry, Sigma-Aldrich Japan or Roche. Chemicals were used without further purification; H_2O was purified by Sartorius filtration system (18.2 Ω) in all experiments.

2.4.2 DNA oligomers

DNA oligomers used in experimental procedures are listed below; all DNA products were purchased from Operon Biotechnologies (Japan).

O1:
5’-GTAATACGACGACTCACTATAGGATCGAAAGATTTCCGC-3’
O2:
5’-ACCTAACGCTAATCCCCTTTCGGGGCCGCGCAAATCTTTCGATC-3’
O3:
5’-ACCTAACGCTAATCCCCT-3’
O4:
5’-GGCGTAATACGACTCACTATAG-3’
O5:
5’-GTAATACGACTCACTATAGGCGGGGTGGAGCAGCCTGGTAGCTCGTCG
G-3’
O6:
5’-GAACCGACGATCTTCGGGTTATGAGCCCGACGAGCTACCAGCCT-3’
O7:
5’-TGGTTGCGGGGGGCCGGATTTGAACCGACGATCTTCGGG-3’
O8:
5’-TGGTTGCGGGGGCCCGATTT-3’
O9:
5’-TAATACGACTCACTATAGGGTTAACTTTAAGAAGGAGATATACATATG-
3’

O10:

5’-TTTCCGCCCCCCGTCCACCGCTGCCACTCCCGCTGCA-3’

NNK4:

5’-ACCGCTGCCACTCCCGCTGCAMNNMNNMNNMNNCATATGTATATCTC
CTTCTTA-3’

NNK5:

5’-ACCGCTGCCACTCCCGCTGCAMNNMNNMNNMNNMNNCATATGTATAT
CTCCTTCTTA-3’

NNK6:

5’-ACCGCTGCCACTCCCGCTGCAMNNMNNMNNMNNMNNMNNCATATGT
ATATCTCCTTCTTA-3’

NNK7:

5’-ACCGCTGCCACTCCCGCTGCAMNNMNNMNNMNNMNNMNNMNNCATA
TGTATATCTCCTTCTTA-3’

NNK8:

5’-ACCGCTGCCACTCCCGCTGCAMNNMNNMNNMNNMNNMNNMNNCATA
TGTATATCTCCTTCTTA-3’

NNK9:

5’-ACCGCTGCCACTCCCGCTGCAMNNMNNMNNMNNMNNMNNMNNMNN
CATATGTATATCTCCTTCTTA-3’

NNK10:

5’-ACCGCTGCCACTCCCGCTGCAMNNMNNMNNMNNMNNMNNMNNMNN
MNNCATATGTATATCTCCTTCTTA-3’

NNK11:

5’-ACCGCTGCCACTCCCGCTGCAMNNMNNMNNMNNMNNMNNMNNMNN
MNNMNNCATATGTATATCTCCTTCTTA-3’

NNK12:

5’-ACCGCTGCCACTCCCGCTGCAMNNMNNMNNMNNMNNMNNMNNMNN
MNNMNNMNNCATATGTATATCTCCTTCTTA-3’

Puromycin linker:

5’-CTCCCGCCCCCCGTCC(SPC18)$_5$CC(Puromycin)-3’ SPC18= spacer 18,hexa-(ethylene glycol) phosphate

2.4.3 FIT system

The methionine-deficient FIT system was used for all in vitro translation. All necessary components for translation were composed in this system as follows: 1.2 μM ribosome; 0.1 μM T7 RNA polymerase; 4.0 μg/mL creatine kinase; 3 μg/mL myokinase; 0.1 μM pyrophosphatase; 0.1 μM nucleotide-diphosphatase kinase; 0.5 mM of all 20 proteinogenic amino acids except for methionine; 0.73 μM AlaRS; 0.03 μM ArgRS; 0.38 μM AsnRS; 0.13 μM AspRS; 0.02 μM CysRS; 0.06 μM GlnRS; 0.23 μM GluRS; 0.02 μM GlyRS; 0.02 μM HisRS; 0.4 μM IleRS; 0.04 μM LeuRS; 0.11 μM LysRS; 0.03 μM MetRS; 0.68 μM PheRS; 0.16 μM proRS; 0.04 μM SerRS; 0.09 μM ThrRS; 0.03 μM TrpRS; 0.02 μM TyrRS;0.02 μM ValRS; 0.6 μM MTF; 2.7 μM IF1; 0.4 μM IF2; 1.5 μM IF3; 0.26 μM EF-G; 10 μM EF-Tu; 10 μM EF-Ts; 0.25 μM RF2; 0.17 μM RF3; 0.5 μM RRF; 1.5 mg/mL E.coli total tRNA; 2 mM ATP; 2 mM GTP; 1 mM CTP; 1 mM UTP; 2 mM spermidine; 20 mM creatine phosphate; 2 mM DTT; 0.1 M 10-forml-5,6,7,8-tetrahydrofolic acid; 50 mM HEPES-KOH (pH7.6); 12 mM magnesium acetate; 100 mM potassium acetate.

2.4.4 Preparation of Flexizyme (eFx)

The eFx was prepared via translation of a DNA template made by a two steps PCR reaction. O1 was annealed with O2 at 1 μM concentration in 1 mL scale and extended using homemade Taq DNA polymerase. 10 μL of extension product was mixed with 2 mL PCR reaction buffer containing 1 μM O3 and O4 as forward and reverse primers and amplified by PCR reaction (approximately 12 to 15 cycles). Then the DNA product was purified via phenol/chloroform extraction and ethanol precipitation. The resulted DNA pellet was resuspended in H_2O and transcribed by homemade T7 RNA polymerase. This transcribed product was eFx and further purified via denaturing PAGE gel electrophoresis. The eFx was extracted from the gel and precipitated by 0.3 M NaCl and ethanol. The eFx pellet was dissolved in H_2O and the concentration was adjusted to 250 μM.

2.4.5 Preparation of $tRNA^{fMet}_{CAU}$

The $tRNA^{fMet}_{CAU}$ was prepared via translation of a DNA template made by PCR reaction in the same manner as eFx. O5 was initially annealed with O6 at 1 μM concentration in 1 mL scale and extended using homemade Taq DNA polymerase. 10 μL of extension product was mixed with 2 mL PCR reaction buffer containing 1 μM O4 and O7 as forward and reverse primers and amplified by PCR reaction (approximately 12 to 15 cycles). In addition, this PCR product was amplified by using O4 and O8 as forward and reverse primers. Then the final DNA product was purified via phenol/chloroform extraction and ethanol precipitation. The purified DNA pellet was resuspended in H_2O and transcribed by homemade T7 RNA polymerase. This transcribed product was $tRNA^{fMet}_{CAU}$ and further purified via denaturing PAGE gel electrophoresis. The $tRNA^{fMet}_{CAU}$ was extracted from the gel and precipitated by 0.3 M NaCl and ethanol. The $tRNA^{fMet}_{CAU}$ pellet was dissolved in H_2O and the concentration was adjusted to 250 μM.

2.4.6 Preparation of mRNA libraries

mRNA libraries were prepared via translation of a series DNA templates made by PCR reactions. NNK (4-12) were annealed with O9, respectively and extended using homemade Taq DNA polymerase. The extension products were PCR amplified using O9 and O10 as forward and reverse primers. Then this PCR product was purified via phenol/chloroform extraction and ethanol precipitation. The purified DNA pellet was resuspended in H_2O, transcribed by homemade T7 RNA polymerase and further purified by denaturing PAGE gel electrophoresis. The mRNA products (NNK 4-12) were dissolved in H_2O and the concentration was adjusted to 20 μM. The prepared NNK mRNA 4-12 were mixed in a ratio of 0.000125: at a final concentration of 10 μM. The mRNAs in this mixture were ligated with puromycin linke.

2.4.7 Preparation of $^{ClAc\text{-}D}Tyr\text{-}tRNA^{fMet}_{CAU}$ assisted by eFx

eFx was mixed with $tRNA^{fMet}_{CAU}$ to a final concentration of 25 μM in 50 mM HEPES-KOH (pH 7.5) with 600 mM $MgCl_2$. This mixture was heated at 95 °C for 2

min, stand at room temperature for 5 min and incubated on ice for another 5 min. Then home made N-chloroacetyl D-Tyrosine cyanomethyl ester dissolved in DMSO was added to a final concentration of 5 mM and incubated one more hour on ice. Then 0.3M sodium acetate (pH 5.2) was added to quench the acylation reaction. The acylated tRNA product was participated and purified by ethanol and the final pellet was dried and dissolved in 1.0 μL of 0.1 mM sodium acetate.

2.4.8 Macrocyclic peptides library design

Two thioether-macrocyclic peptide libraries were constructed with either *N*-(2-chloroacetyl)-L-tyrosine ($ClAc^{L}Y$) or *N*-(2-chloroacetyl)-D-tyrosine ($ClAc^{D}Y$) as an initiator by using the Flexible in vitro Translation (FIT) system. The corresponding mRNA library is designed to have an AUG ($ClAc^{L/D}Y$) initiator codon followed by 4-12 NNK random codons which code random proteinogenic amino acids and C-terminus UGC (Cys) codon. Therefore the diversity of the macrocycles is up to 10^{12}. After *in vitro* translation, a thioether bond formed spontaneously between the N-terminal ClAc group of the initiator $^{L/D}$Tyr residue and the sulfhydryl group of a downstream Cys residue. It should be noted that the macrocyclic molecules with a $ClAc^{L}Y$ or $ClAc^{D}Y$ initiator would potentially form altered tertiary structural conformation.

2.4.9 Preparation of *B. malayi* iPGM and PGM enzymes

The His_{10}-tagged *B. malayi* iPGM for the selection and PGM enzymes in activity assay were all from my collaborator Doctor. Zhiru Li in New England Biolabs, USA. They cloned all PGM enzymes into pET21a(+), expressed in the *Escherichia coli* strain C2566/T7 Express and purified. The production of soluble recombinant enzymes were optimized at 37 °C. After the OD600 reached 0.6, 0.1 mM IPTG was added for induction. The mixture containing His-tagged enzymes was subject to 5 ml HiTrap™ chelating HP column (GE Healthcare; Pittsburg, PA) and purified via an AKTA FPLC following manufacturer's instructions. The sample was applied to the column and washed with five column volumes of buffer A (20 mM NaPO4, 300 mM NaCl, 10 mM imidazole pH 7.4). Protein was then eluted using a linear gradient

(8–100%) of buffer B equivalent to 40–400 mM imidazole. Purity of the protein was estimated by 4–20% SDS–PAGE and the protein concentration was determined using the Bradford assay.[2,5,6]

2.4.10 Affinity selection of Bm iPGM binding macrocyclic peptides

Affinity selections were performed with ^{D}Tyrosine library against *B. malayi* iPGM (His_{10}-tagged) by employing the RaPID system.[7] The mRNA library, ClAc-D-Tyr-$tRNA^{fMet}_{CAU}$ was prepared as reported.[8,9] 1 μM mRNAs library were ligated with 1.5 μM puromycin linker using a T4 RNA ligase at 25 °C for 30 min and purified. Then, 1.4 μM mRNA-puromycin conjugate and 50 μM ClAc-^{D}-Tyr-$tRNA^{fMet}_{CAU}$ was used in a methionine-deficient FIT system to generate peptide libraries. The in vitro translation reaction were performed at 37 °C for 30 min with an extra incubation at 25 °C. After an addition of EDTA solution (200 mM, 15 μL), the reaction solution was incubated at 37 °C for 30 min to facilitate thioether cyclization and subject to pre-washed Sephadex G-25 columns to remove salts. The desalted solution of peptide-mRNA was applied to Dynabeads His-tag Isolation & Pulldown magnetic beads (Invitrogen) to remove undesired beads binders. This process is called pre-clearance and was repeated twice. After pre-clearance, the peptide-mRNA solution was incubated with *B. malayi* iPGM-immobilized Dynabeads for 30 min at 4 °C to obtain iPGM-binders. This process referred to as positive selection. The selected fused peptide-mRNAs on the beads were reverse transcribed by M-MLV reverse transcriptase (Promega) for 1 h at 42 °C. The fused peptide-cDNAs were isolated from the beads by using in 1×PCR reaction buffer and heated 5 min at 95 °C. The amount of eluted cDNAs was measured by quantitative PCR (qPCR). The remained cDNAs were amplified by PCR, purified and transcribed into mRNAs as a library for the next round of selection. The library preparation, preclearance and positive selection were one round of the enrichment processes. Significant cDNAs enrichments were observed at the sixth round for *B. malayi* iPGM, respectively. The recovered cDNAs were ligated into the pGEM-T-Easy cloning vector (Promega), using TA-cloning. The vectors were transformed into DH5α competent cells, individual clones were picked, PCR amplified and sequenced.

2.4.11 Fmoc solid phase peptide synthesis (SPPS) and HPLC purification

All peptides were chemically synthesized (25 μmole scale) using a Syro Wave automated peptide synthesizer (Biotage) by Fmoc SPPS. Firstly, NovaPEG Rink Amide resins (25 μmole scale) were incubated with N,N-dimethylformamide (DMF) with rotation at ambient temperature for 30 min and washed with DMF (1 mL, 5 times). Coupling of each Fmoc-protected amino acid was performed on the engorged resin with a solution of 300 μL 0.5 M Fmoc-protected amino acid 300 μL 0.5 M 2-(1H-Benzotriazole-1-yl)-1,1,3,3-tetramethyluronium hexafluorophosphate (HBTU) and 1-hydroxybenzotriazole (HOBt), and 150 μL 0.5 M N,N-diisopropylethylamine (DIPEA) in DMF and reacted for 1 hour at ambient temperature. After washing the resins with DMF (1 mL, 5 times), Fmoc-deprotection was performed by incubating the resin with 600 μL of 40% piperidine in DMF (vol/vol) and reacted for 30 min at ambient temperature. Each peptide was synthesized using the appropriately protected amino acid monomers corresponding to sequences in Tables 1 and 2 by repeating the Fmoc-protected amino acid coupling and Fmoc-deprotection steps accordingly. The N-terminal α-amino group of the synthesized peptides on the resin was chloroacetylated by incubating with a solution of 500 μL 0.5 M chloroacetyl N-hydroxysuccinimide (NHS) ester in N-methylpyrrolidone (NMP) with rotation for 60 min at ambient temperature. For the synthesis of Ce-L2 and Ce-L2d, the N-terminal α-amino group was acetylated by incubating with a solution of 500 μL 0.5 M acetic anhydride and 0.25 M DIPEA in NMP with rotation for 60 min at ambient temperature. After washing the resin with DMF (1 mL, 5 times), peptides were fully deprotected and cleaved from resin by incubating with a solution of 2 mL trifluoroacetic acid (TFA), water, triisopropylsilane (TIS) and ethanedithiol (EDT) (92.5:2.5:2.5:2.5) with rotation for 3 hours at ambient temperature and precipitated with diethyl ether. The peptide pellet was dissolved in 10 mL DMSO/0.1%TFA in water (1:1), and the pH adjusted to >8 by addition of triethylamine (TEA), and incubate at ambient temperature for 1 h to enhance the cyclization via a thioether bond formation between N-terminal chloroacetamide group and cysteine sulfhydryl group. Peptide mass and cyclization was confirmed by MALDI-TOF MS analysis. The cyclization reaction was quenched by addition of TFA to acidify the peptide suspensions. Peptides were then purified by reverse-phase HPLC, molecular masses

were verified by MALDI-TOF MS analysis, using a microflex or autoflex instrument (Bruker Daltonics).

2.4.12 iPGM and dPGM assays

Inhibitory assays were performed in collaboration with Prof. James Inglese at National Center for Advancing Translational Sciences, National Institutes of Health in USA. Either a continuous or endpoint output assay was used to measure the phosphoglycerate mutase. For the continuous measurement, the conversion of 3-phosphoglycerate to 2-phosphoglycerate was measured via monitoring the consumption of NADH by a coupled enzyme reaction. the oxidation of NADH via lactate dehydrogenase was monitored at an absorbance of 340 nM.[6,10,11]

2.5 References

1 Taylor, M. J., Hoerauf, A. & Bockarie, M. Lymphatic filariasis and onchocerciasis. *The Lancet* **376**, 1175-1185 (2010).

2 Zhang, Y., Foster, J. M., Kumar, S., Fougere, M. & Carlow, C. K. S. Cofactor-independent phosphoglycerate mutase has an essential role in Caenorhabditis elegans and is conserved in parasitic nematodes. *Journal of Biological Chemistry* **279**, 37185-37190 (2004).

3 Singh, P. K., Kushwaha, S., Mohd, S., Pathak, M. & Misra-Bhattacharya, S. In vitro gene silencing of independent phosphoglycerate mutase (iPGM) in the filarial parasite Brugia malayi. *Infectious Diseases of Poverty* **2**, 1 (2013).

4 Crowther, G. J. *et al.* Cofactor-independent phosphoglycerate mutase from nematodes has limited druggability, as revealed by two high-throughput screens. *PLoS Negl Trop Dis* **8**, e2628 (2014).

5 Raverdy, S., Zhang, Y., Foster, J. & Carlow, C. K. S. Molecular and biochemical characterization of nematode cofactor independent phosphoglycerate mutases. *Molecular and biochemical parasitology* **156**, 210-216 (2007).

6 White, M. F. & Fothergill‐Gilmore, L. A. Development of a mutagenesis, expression and purification system for yeast phosphoglycerate mutase. *European Journal of Biochemistry* **207**, 709-714 (1992).

7 Yamagishi, Y. *et al.* Natural product-like macrocyclic N-methyl-peptide inhibitors against a ubiquitin ligase uncovered from a ribosome-expressed de novo library. *Chemistry & biology* **18**, 1562-1570 (2011).

8 Hayashi, Y., Morimoto, J. & Suga, H. In vitro selection of anti-Akt2 thioether-macrocyclic peptides leading to isoform-selective inhibitors. *ACS chemical biology* **7**, 607-613 (2012).

9 Hipolito, C. J., Tanaka, Y., Katoh, T., Nureki, O. & Suga, H. A macrocyclic peptide that serves as a cocrystallization ligand and inhibits the function of a MATE family transporter. *Molecules* **18**, 10514-10530 (2013).

10 Feraudi, M., Gärtner, C., Kolb, J. & Weicker, H. Bioluminescent and

Fluorometric Techniques for Determinations of 19 Metabolites of ADP/ATP-Dependent Transformations in Energy Metabolism in 200 (or 400) mg Muscle. *Clinical Chemistry and Laboratory Medicine* **21**, 193-198 (1983).

11 Fuad, F. A. A. *et al.* Phosphoglycerate mutase from Trypanosoma brucei is hyperactivated by cobalt in vitro, but not in vivo. *Metallomics* **3**, 1310-1317 (2011).

Chapter 3

Development of macrocyclic peptide inhibitors against *C. elegans* iPGM

3.1 Introduction

Caenorhabditis elegans (*C. elegans*) is small (~1mm in length) free-living nematode with transparent body and lives in soil environment.[1,2] *C. elegans* has been utilized as a model organism for the first time to investigate neural development in animals. Furthermore, genetic pathways and cellular processes were well studied via *C. elegans*, including cell death and aging.[3-5]

Recently, iPGM enzyme from *C. elegans* have been cloned, purified and well characterized. *C. elegans* iPGM was identified as an essential enzyme to catalyze the conversion of 3-PG and 2-PG and proved to be crucial for the development of *C. elegans* by RNAi study which is a powerful technology to evaluate function of genes and encoded proteins.[6,7,8] Since *C. elegans* iPGM shares high conservation of primary sequences of the catalytic residues with iPGMs from parasitic nematodes and bacteria, including *Brugia malayi* (*B. malayi* iPGM), *Onchocerca volvulus* (*O. volvulus* iPGM), *Dirofilaria immitis* (*D. immitis* iPGM), and *Escherichia Coli* (*E. coli* iPGM). Thus, *C. elegans* iPGM is considered as a promising drug target for the discovery of novel molecules with anti-parasite activity, which could be developed as potential lead compounds for treatment of parasitic diseases.

To discover macrocyclic peptide inhibitors with potent and broad-spectrum inhibitory activity toward iPGMs, *in vitro* affinity selection was performed against *C. elegans* iPGM in this chapter.

3.2 Results and discussion

3.2.1 *In vitro* affinity selection against *C. elegans* iPGM

I attempted to discover macrocyclic peptide inhibitors against *C. elegans* iPGM by using the RaPID system. *C. elegans* iPGM (His_{10}-tagged) was employed as target protein and immobilized onto magnetic beads (His-tag Isolation & Pulldown Dynabeads). Two macrocyclic peptide library were constructed with L or D isomers of *N*-chloroacetyl-Tyrosine initiator amino acid, followed by 4~12 random amino acids region and a cysteine residue embedded at the C-terminus. The respective libraries were referred as ^{L}Y- and ^{D}Y-library.

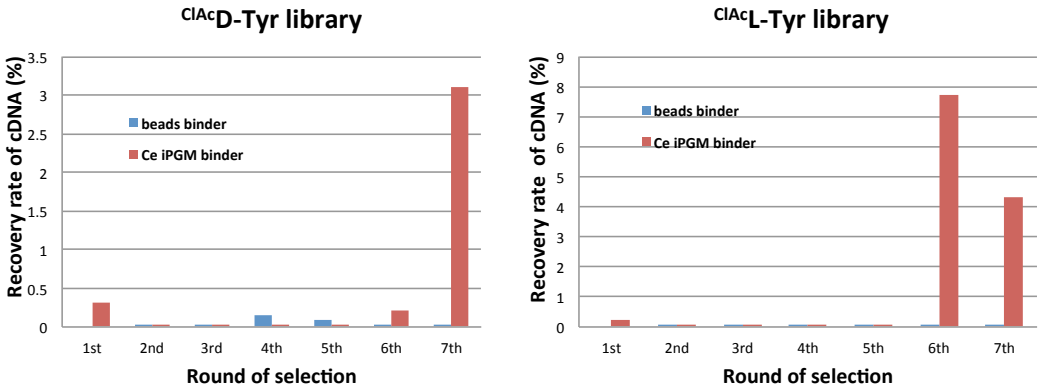

Figure 3-1. The enrichment of *C. elegans* iPGM binding peptides is represented by the recovery rate of cDNA amount in each round of selection. Red bars and blue bars represented the quantity of cDNA from magnetic beads and *C. elegans* immobilized beads, respectively.

The ^{L}Y- and ^{D}Y-libraries were independently incubated with magnetic beads (up to 9 times) to remove non-specific beads binding peptides. Then, the library fraction was applied to *C. elegans* iPGM immobilized beads to select specific target binding peptides. After six rounds of selection, an enrichment of *C. elegans* iPGM binding peptides was observed by monitoring cDNA recovery by RT-PCR, while non-specific binding was significantly suppressed (Figure 3-1). The recovered cDNAs from enriched rounds were analyzed by TA-cloning and sequencing.

Table 3-1. The peptide sequences of the random region derived from recovered cDNA

Sequence	Frequency
DYPGDHCYLYGT	22/45
DYPGDYCYLYGT	3/45
HCHHPVTCT	1/45
PHCHRFKQTSN	1/45
HHRCLFVLCT	1/45
HCHNGIVTLTYY	1/45
LCHHDLPSF	1/45
RCHYRYLI	1/45
LKGHYLFVCVV	1/45
IAYVYKCPHHFN	1/45
NGASIKHCH	1/45
TDSWHIVWHH	1/45
HCNWAQNL	1/45
THRKICLHLPY	1/45
LVNEWPCKRHHQ	1/45
HKRRAGPTCHKP	1/45
ATCNLPRHHNRT	1/45
GIRFTKHPFHRH	1/45
EHNLKCVFHT	1/45
RYANHRYMPRCT	1/45
HHWRINCV	1/45

Sequence	Frequency
ITLANPFRILH	18/22
TTLANPFRILH	1/22
RNTHLRHKPRANCG	1/22
RRAVRCSH	1/22
LEIPTHYINC	1/22

After sequence analysis of isolated peptide, a total of 45 peptides were obtained from ^{D}Y-library (Table 3-1, left), two macrocyclic peptides were identified as *C. elegans* iPGM binding peptides, referred to as Ce-1 and Ce-2. Ce-1 and Ce-2 were found 22 and 3 times in 45 clones, respectively. Both peptides comprise of 15 residues with one amino acid difference at position 7 and have lariat-like structure with head cyclic part and linear tail part (Table 3-2). On the other hand, 22 peptide clones were selected from ^{L}Y-library. Among all identified peptides, Ce-3 was the dominated peptide found 18 times in 22 clones (Table 3-1, right). Ce-4 appeared once in 22 clones and consists of similar sequence with Ce-3 with only one amino acid difference at the

second position. Both Ce-3 and Ce-4 are macrocyclic peptide with short tail and single amino acid difference at position 2 (Table 3-2). This observation implied that the peptides possess different conformational sequence from respective ^{L}Y-and ^{D}Y-libraries. These macrocyclic peptides were chemically synthesized and purified by reverse phase HPLC for binding affinity and inhibitory activity assays. The lariat structure of Ce-2 was confirmed by MSMS spectrum and fragment analysis (Figure 3-16).

Table 3-2. The full-length peptide sequences derived from *in vitro* affinity selection. Ce-1~2 and Ce-3~4 are from ^{L}Y- and ^{D}Y-libraries, respectively.

Peptide ID	Sequence	Ring size/tail length
Ce-1	Ac-^{D}YDYPGDHCYLYGTCG (S–S)	8/7
Ce-2	Ac-^{D}YDYPGDYCYLYGTCG (S–S)	8/7
Ce-3	Ac-^{L}YITLANPFRILHCG (S–S)	13/1
Ce-4	Ac-^{L}YTTLANPFRILHCG (S–S)	13/1

3.2.2 Characterization of selected anti-*C. elegans* iPGM macrocyclic peptides

3.2.2.1 Determination of peptide binding affinity against C. elegans iPGM

All peptides were chemically synthesized by Fmoc solid-phase peptide synthesis method and purified for the binding affinity study against *C. elegans* iPGM. Their kinetic properties were determined by means of surface plasmon resonance (SPR) using Biacore T100 instrument.

All four peptides showed k_a (association rate) values with a range of 1.18-37.8 × 10^6 $M^{-1}s^{-1}$, k_d (dissociation rate) values with a range of 1.31-14.35 × 10^{-3} s^{-1}, resulting in K_D (dissociation constants) with 3.1 to 6.3 nM range (Table 3-3, Figure 3-2). Thus, peptides studied here exhibit remarkable strong binding affinity against *C. elegans* iPGM. Ce-1 showed low dissociation constant (K_D = 6.3 nM) and slow dissociation rate (k_d = 14.35 × 10^{-3} s^{-1}). Ce-2 showed lower dissociation constant (K_D = 4.9 nM) than Ce-1, which may result of its slower dissociation rate (k_d = 1.31 × 10^{-3} s^{-1}). The Tyr7 residue in Ce-2 positively contributes to the binding activity than His7 residue in Ce-1. The one amino acid difference at the second position of Ce-3 and Ce-4 has slightly effect on the binding activity. Ce-3 and Ce-4 revealed dissociation constant of 3.1 and 3.8 nM, respectively. Macrocyclic peptides with short tail like Ce-3 and Ce-4 exhibit higher binding activity against *C. elegans* iPGM than lariat-like cyclic peptides Ce-1 and Ce-2.

Table 3-3. The binding affinity of selected macrocyclic peptides against *C. elegans* iPGM.

Peptide ID	Sequence	k_a (×10^6 $M^{-1}s^{-1}$)	k_d (×10^{-3} s^{-1})	K_D (nM)
Ce-1	Ac-DYDYPGDHCYLYGTCG (S–S)	2.28	14.35	6.3
Ce-2	Ac-DYDYPGDYCYLYGTCG (S–S)	2.69	1.31	4.9
Ce-3	Ac-LYITLANPFRILHCG (S–S)	1.18	3.69	3.1
Ce-4	Ac-LYTTLANPFRILHCG (S–S)	3.78	1.46	3.8

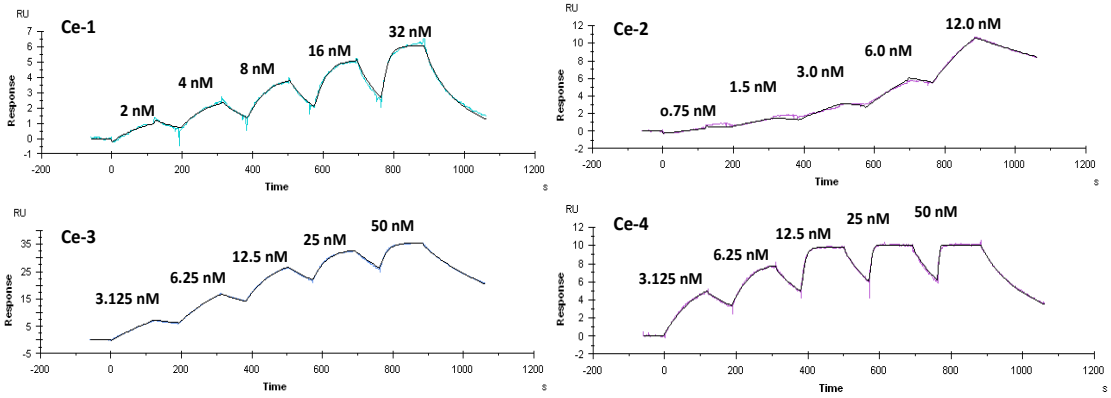

Figure 3-2. SPR sensorgrams of Ce-1, Ce-2, Ce-3 and Ce-4 against C. elegans iPGM measured by the Biacore T100 instrument. The measurements were performed by single-cycle kinetic mode with five peptide concentrations.

3.2.2.2 Evaluation of peptide inhibitory activity against *C. elegans* iPGM

The inhibitory activities of identified peptides were evaluated against iPGMs orthologs from *B. malayi*, *C. elegans*, *O. volvulus*, *D. immitis* and *E. coli* and dPGM isozymes from human and bacteria by an enzyme-coupled bioluminescent assay described in chapter 2.

The results showed that all tested peptides act as *C. elegans* iPGM inhibitors that prevent the catalytic activity of iPGM (Table 3-4). Ce-1 and Ce-2 completely shut down the mutase activity of *C. elegans* iPGM (Figure 3-3) with pIC_{50} of 8.40 and 8.65 (IC_{50} = 4.0 and 2.2 nM). The K_D values of Ce-1 and Ce-2 determined by SPR analysis well reflected their inhibitory activities against *C. elegans* iPGM. Although Ce-3 and Ce-4 exhibit high binding affinity with K_D values of 3.1 and 3.8 nM in SPR studies, they displayed weaker inhibitory activity with pIC_{50} of 6.33 and 5.22 (IC_{50} = 0.47 and 6.0 μM) and the inhibition potency drop 100 and 1000 folds, comparing with Ce-1 and Ce-2. This observation indicated that Ce-1~2 with lariat-like structure and Ce-3~4 with macrocyclic structure might have different inhibitory mechanisms. It is assumed that the constrained cyclic structure in Ce-1 and Ce-2 assisted the recognition of binding site, and the flexible linear residues greatly contribute to the

inhibitory activity. This speculation was examined by a series of structure activity study in the next chapter. Furthermore, dPGMs were not inhibited and retained catalytic activity. This result showed the isoform selective ability of selected macrocyclic peptides to dPGM.

The inhibitory activity of peptides is also tested against iPGM orthologs from parasites and bacteria， including *B. malayi*, *O. volvulus*, *D. immitis* and *E. coli*. (Table 3-4). Ce-1 and Ce-2 exhibit broad-spectrum inhibitory activity against all iPGM orthologs. Ce-1 displayed pIC_{50} values with a range of 8.38-7.62 (IC_{50} 4.0-24.0 nM). Ce-2 is more potent inhibitor with pIC_{50} values with a range of 8.78-7.72 (IC_{50} 1.7-19.0 nM). On the other hand, Ce-3 and Ce-4 can inhibit *C. elegans* iPGM and *E. coli*. iPGM, but the inhibitory ability is not as potent as Ce-1~2. Ce-1~2 represent the first iPGM inhibitors with low nM activity (IC_{50} 4.0-24.0 nM) and broad-spectrum inhibitory activity. Comparing to Ce-3~4, Ce-1~2 have lariat-like structure with cyclic head and linear tail sequence, the function of these two parts were extensively analyzed by structure activity relationship studies on Ce-2.

Table 3-4. The inhibitory activity of selected macrocyclic peptides against target enzyme *B. malayi* iPGM and four iPGM orthologs from *C. elegans*, *O. volvulus*, *D. immitis* and *E. coli*, two PGM isozymes from *E. coli* and *H. sapiens*

Peptide ID	Sequence	pIC_{50}						
		B.malayi iPGM	C. elegans iPGM	O. volvulus iPGM	D. immitis iPGM	E. coli iPGM	E. Coli dPGM	H. sapiens dPGM
Ce-1	Ac-DYDYPGDHCYLYGTCG (S–S)	7.92	8.40	7.62	8.04	8.38	NA	NA
Ce-2	Ac-DYDYPGDYCYLYGTCG (S–S)	8.27	8.65	7.72	8.21	8.78	NA	NA
Ce-3	Ac-LYITLANPFRILHCG (S–S)	NA	6.33	NA	NA	6.27	NA	NA
Ce-4	Ac-LYTTLANPFRILHCG (S–S)	NA	5.22	NA	NA	5.28	NA	NA

pIC_{50}= -log IC_{50}, ex. pIC_{50}=9 equal $IC_{50}=10^{-9}$ M. NA = No appreciable inhibitory activity at highest concentration tested,

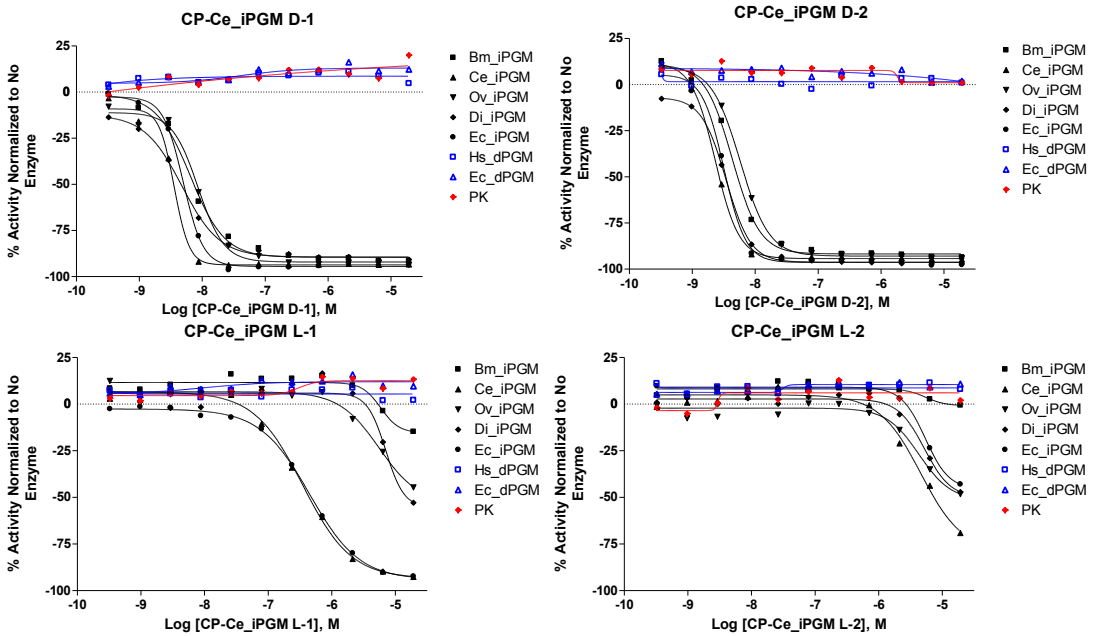

Figure 3-3. IC_{50} concentration-response curves for characterization of Ce-1 to Ce-4 on the iPGM orthologs and dPGM isozymes using the enzyme coupled bioluminescent assay.

3.2.3 Structure activity relationship studies of Ce-2

Ce-2 has a lariat-like structure with cyclic head (8 amino acids) and linear tail (7 amino acids) and exhibit potent iPGM inhibitory activity. Ce-2 was chosen as a template for further structure activity relationship studies in this section. A series of chemical modification were performed including C-terminal truncation to explore the minimal sequence for activity and N-methyl scanning to improve biological properties.

3.2.3.1 Truncation study on Ce-2 tail peptide

The function of Ce-2 tail peptide was firstly studied by preparing seven C-terminal truncated analogs Ce-2-1 to Ce-2-7 (Table 3-5). Truncated analogs have tail peptide with various lengths. The binding affinities of truncated analogs were determined by SPR experiment (Table 3-5). Truncated analogs Ce-2-1 to Ce-2-5 showed high binding affinity (K_D = 1.9-14.4 nM) as parent peptide Ce-2 (K_D = 4.9 nM). But, Ce-2-6 with one tail residue and Ce-2-7 without tail resulted in loss binding affinity towards *C. elegans* iPGM, indicating the importance of tail peptide for binding.

Table 3-5. The binding affinity of truncated Ce-2 peptide analogs against *C. elegans* iPGM.

Peptide ID	Sequence	k_a ($\times 10^6$ $M^{-1}s^{-1}$)	k_d ($\times 10^{-3}$ s^{-1})	K_D (nM)
Ce-2	Ac-D(S)YDYPGDYCYLYGTCG	2.69	1.31	4.9
Ce-2-1	Ac-D(S)YDYPGDYCYLYGTC	1.46	3.65	4.9
Ce-2-2	Ac-D(S)YDYPGDYCYLYGT	12.0	1.73	14.4
Ce-2-3	Ac-D(S)YDYPGDYCYLYG	4.98	14.9	3.0
Ce-2-4	Ac-D(S)YDYPGDYCYLY	1.17	2.22	1.9
Ce-2-5	Ac-D(S)YDYPGDYCYL	2.48	7.23	2.9
Ce-2-6	Ac-D(S)YDYPGDYCY	N.D.	N.D.	N.D.
Ce-2-7	Ac-D(S)YDYPGDYC	N.D.	N.D.	N.D.

N.D.= Not detected in Biacore instrument.

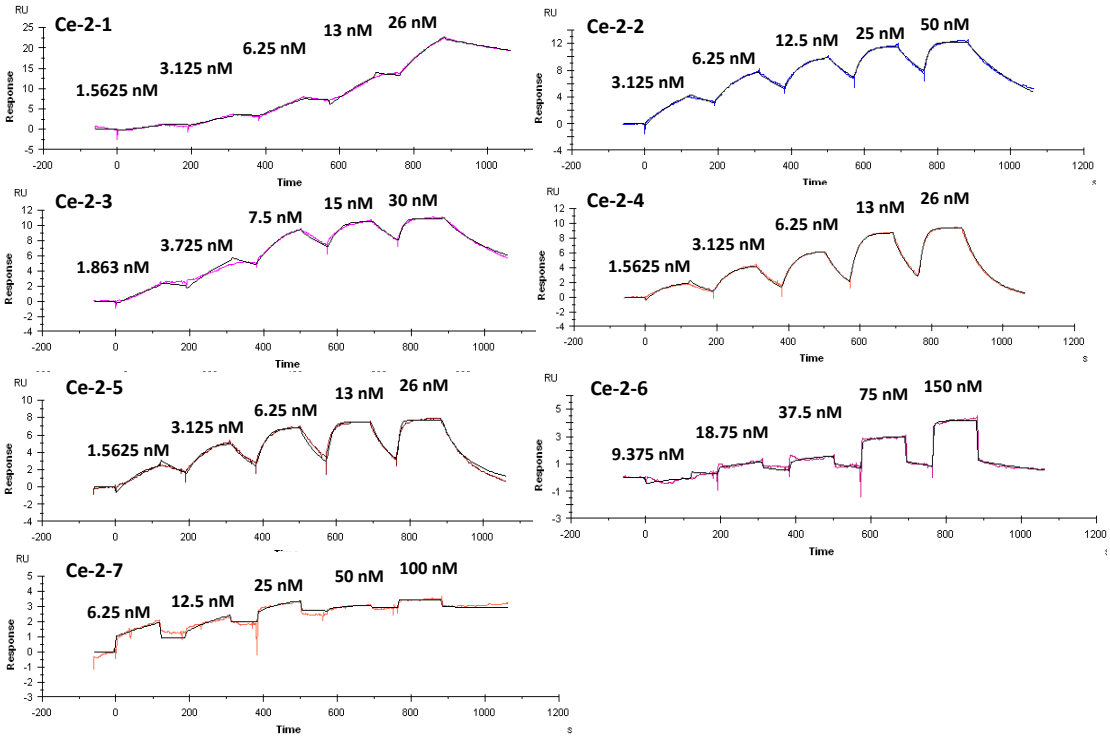

Figure 3-4. SPR sensorgrams of truncated Ce-2 analogs against *C. elegans* iPGM measured by the Biacore T100 instrument. The measurements were performed by single-cycle kinetic mode with five peptide concentrations.

The inhibitory activities of truncated analogs were also evaluated (Table 3-6). Ce-2-1 retained activity as Ce-2. The inhibitory activities of Ce-2-2 to Ce-2-5 decreased slightly against *C. elegans* iPGM. The inhibition assay suggests that the deletion of the terminal Cysteine residue resulted in a loss of activity for broad spectrum toward iPGM orthologs, where only *C. elegans* iPGM and *E. coli* iPGM could be inhibited by this Cysteine-deleted peptide. Further truncation of the tail peptide had also a similar effect, complete deletion of the tail peptide resulted in total loss of inhibitory activity and binding affinity. These results indicated that the tail peptide does not only contribute to binding to *C. elegans* iPGM, but plays critical roles in exhibiting inhibitory function as well as a broad spectrum of inhibitory activity.

Table 3-6. The inhibitory activity of truncated Ce-2 analogs against target enzyme *C. elegans* iPGM and four iPGM orthologs from *B. malayi*, *O. volvulus*, *D. immitis* and *E. coli*, two dPGM isozyme from *E. coli* and *H. sapiens*

Peptide ID	Sequence	pIC_{50}						
		B. malayi iPGM	C. elegans iPGM	O. volvulus iPGM	D. immitis iPGM	E. coli iPGM	E. coli dPGM	H. sapiens dPGM
Ce-2	Ac-DYDYPGDYCYLYGTCG (S–S)	8.27	8.65	7.72	8.21	8.78	NA	NA
Ce-2-1	Ac-DYDYPGDYCYLYGTC (S–S)	8.07	8.39	7.31	7.82	8.51	NA	NA
Ce-2-2	Ac-DYDYPGDYCYLYGT (S–S)	6.16	7.80	5.61	5.96	7.98	NA	NA
Ce-2-3	Ac-DYDYPGDYCYLYG (S–S)	5.93	7.64	5.41	5.7	7.98	NA	NA
Ce-2-4	Ac-DYDYPGDYCYLY (S–S)	7.17	8.56	6.72	7.04	8.71	NA	NA
Ce-2-5	Ac-DYDYPGDYCYL (S–S)	5.53	7.16	4.72	5.32	7.27	NA	NA
Ce-2-6	Ac-DYDYPGDYCY (S–S)	NA	NA	NA	NA	NA	NA	NA
Ce-2-7	Ac-DYDYPGDYC (S–S)	NA	NA	NA	NA	NA	NA	NA

pIC_{50}= -log IC_{50}, ex. pIC_{50}=9 equal $IC_{50}=10^{-9}$ M. NA = No appreciable inhibitory activity at highest concentration tested.

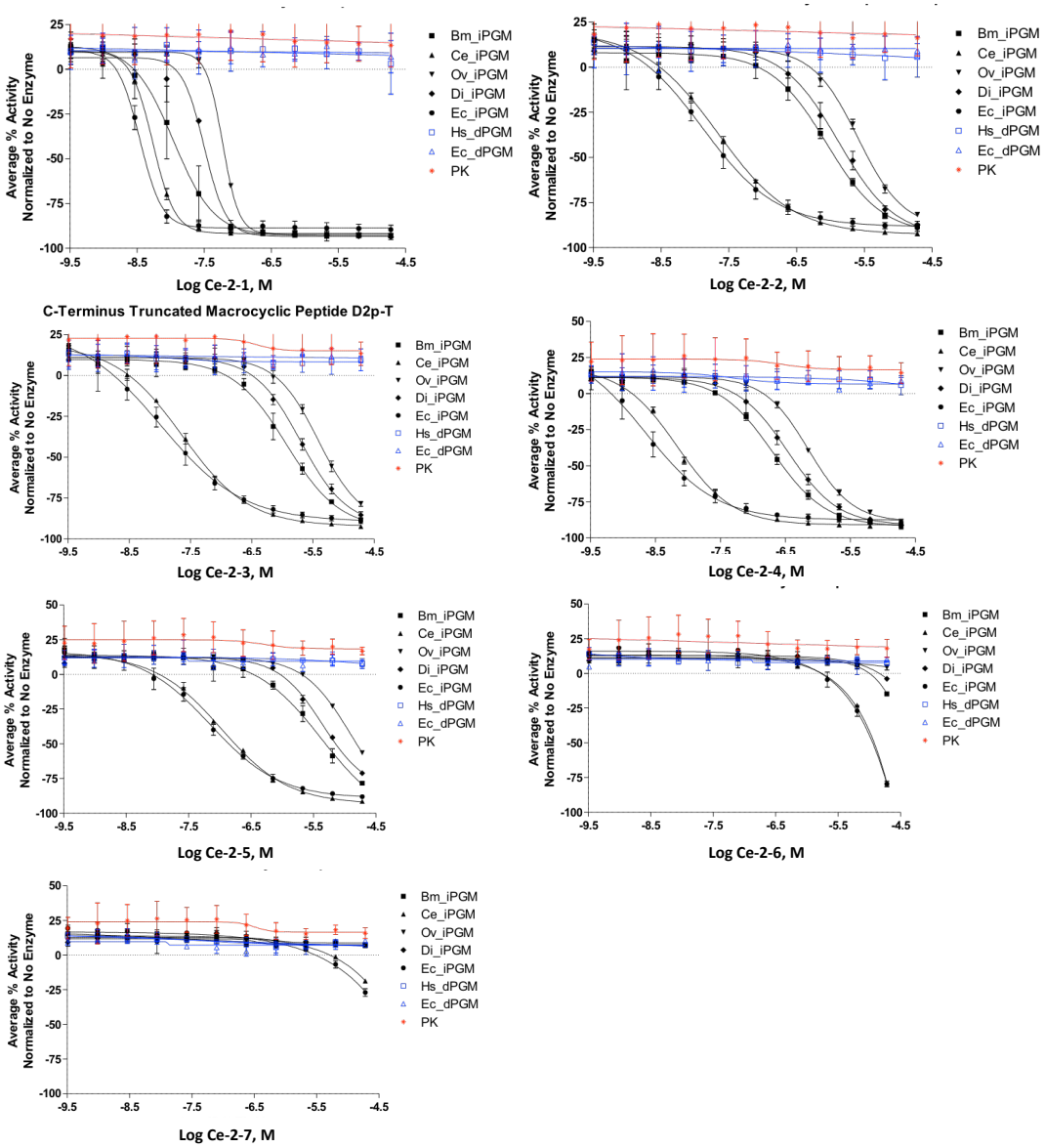

Figure 3-5. IC_{50} concentration-response curves for characterization of truncated Ce-2 analogs on the iPGM orthologs and dPGM isozymes using the enzyme coupled bioluminescent assay.

On the other hand, the macrocyclic structure of peptide might contribute to improve target-binging affinity by preorganizing the structure of cyclic peptide. To examine the importance of macrocyclic structure, two linear analogs of Ce-2 were synthesized. Ce-L2 and Ce-L2-4 are linear peptide counterparts derived from Ce-2 and Ce-2-4, respectively by altering *N*-terminal chloroacetyl group (ClAc) to an acetyl group (Ac) in initiator Tyrosine residue and replacing Cys8 to Ser (Table 3-7). Again, the binding affinity and inhibitory activity were determined.

Ce-L2 showed 30-fold slower association rate (k_a) and 100-fold faster dissociation rate (k_d) from *C. elegans* iPGM than Ce-2. The binding affinity and inhibitory activity of Ce-L2 decreased 30-folds (K_D = 138.9 nM) and 500-folds (pIC50 = 5.94, IC50 = 1.1 μM), comparing to Ce-2 (K_D = 4.9 nM, pIC50 = 8.65, IC50 = 2.2 nM). On the other hand, Ce-L2-4 completely lost binding and inhibitory activity, implying that macrocyclic structure improved target affinity significantly and C-terminal GTCG residues contribute to binding activity for linear analogs.

In addition, to evaluate the function of tail peptide in Ce-2, a linear analog representing the tail residues of Ce-2 was synthesized (Table 3-7). The binding and inhibitory activities were also verified toward *C. elegans* iPGM. Interestingly, Ce-2tail showed no bind and inhibitory activity, indicating that tail peptide might act together with cyclic head for biological activity. Thus, both cyclic head and linear tail in Ce-2 are essential features to maintain the full binding and inhibitory activity.

Table 3-7. The binding affinity and inhibitory activity of linear Ce-2 analogs against C. elegans iPGM

Peptide ID	Sequence	K_a ($\times 10^6$ $M^{-1}s^{-1}$)	k_d ($\times 10^{-3}$ s^{-1})	K_D (nM)	pIC_{50}
Ce-2	Ac-DYDYPGDYCYLYGTCG (S–S)	2.69	1.31	4.9	8.65
Ce-L2	Ac-DYDYPGDYSYLYGTCG	76.0	105.3	138.6	5.94
Ce-L2-4	Ac-DYDYPGDYSYLY	N.D.	N.D.	N.D.	NA
Ce-2tail	Ac-LYLYGTCG	N.D.	N.D.	N.D.	NA

pIC_{50} = -log IC_{50}, ex. pIC_{50}=9 equal IC_{50}=10^{-9} M. N.D. = Not detected in Biacore instrument, NA = No appreciable inhibitory activity at highest concentration

3.2.3.2 Study of C-terminal Cysteine by substitution modification

The deletion of C-terminal cysteine resulted in loss of broad-spectrum activity. To verify if the C-terminal cys14 can be substituted with redox active sidechain and the effect of sidechain on activity, I also prepared a set of macrocyclic peptides of Ce-2 with C-terminal modifications with either DOPA (Ce-2D1 and Ce-2D2) or Serine (Ce-2S) (Table 3-8). Based on our past knowledge that DOPA-like catechol moiety exhibited low inhibitory activity (~high μM) against iPGMs. Again, these peptides were chemically synthesized and tested for binding affinity and inhibitory assay.

The kinetic and dissociation constants were determined by means of SPR against *C. elegans* iPGM (His_{10}-tagged) immobilized on NTA-sensor chip. All peptide analogs showed values of K_D with a range of 2.38-7.58 nM (Table 3-8). The dissociation constants of all peptides revealed no significant change comparing to parent Ce-2, implying that substitution of C-terminal cys14 did not lead to dramatic effect on the binding ability toward *C. elegans* iPGM.

Table 3-8. The binding affinity Ce-2 analogs against *C. elegans* iPGM

Peptide ID	Sequence	K_a ($\times 10^6$ $M^{-1}s^{-1}$)	k_d ($\times 10^{-3}$ s^{-1})	K_D (nM)
Ce-2	Ac-DYDYPGDYCYLYGTCG (S–S)	2.69	1.31	4.9
Ce-2S	Ac-DYDYPGDYCYLYGTSG (S–S)	2.04	4.86	2.38
Ce-2-D1	Ac-DYDYPGDHCYLYGT(X) (S–S)	4.6	3.49	7.58
Ce-2-D2	Ac-DYDYPGDHCYLYG(X) (S–S)	1.06	3.3	3.12

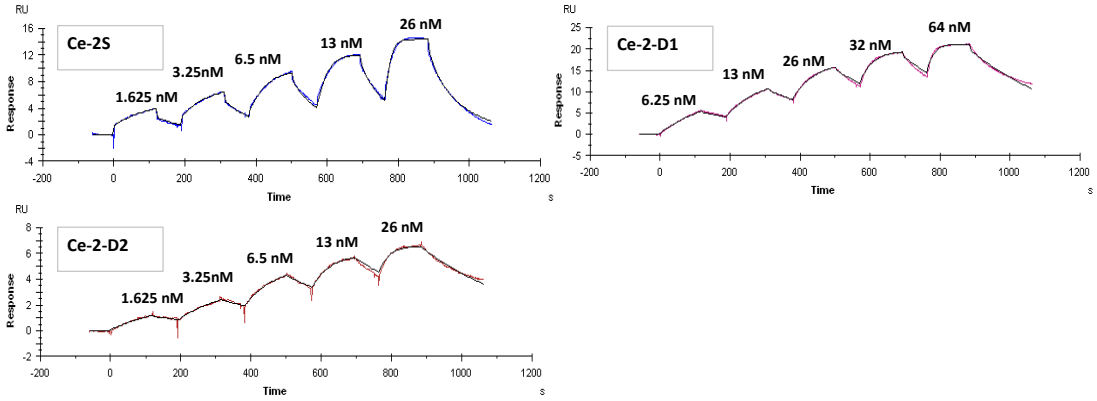

Figure 3-6. SPR sensorgrams of truncated Ce-2 analogs against *C. elegans* iPGM measured by the Biacore T100 instrument. The measurements were performed by single-cycle kinetic mode with five peptide concentrations.

Although C-terminal substituted analogs were still tight *C. elegans* iPGM binders, it does not mean that they are able to inhibit iPGMs. Thus, it is necessary to test the inhibitory activities. The substitution of the C-terminal cys14 residue with DOPA resulted in loss of inhibitory activity with 50-fold against *C. elegans* iPGM and >100-fold for other iPGMs (Table 3-9). On the other hand, Ce-2S, a C-terminal Ser-modification analog remains active against *C. elegans* and *E. coli* iPGMs. This observation suggests that the C-terminal cys14 plays crucial role to maintain potent and broad-spectrum inhibitory activity.

Table 3-9. The inhibitory activity of Ce-2 analogs against iPGM orthologs and dPGM isozyme.

Peptide ID	Sequence	pIC_{50}						
		C. elegans iPGM	*B. malayi* iPGM	*O. volvulus* iPGM	*D. immitis* iPGM	*E. coli* iPGM	*E. coli* dPGM	*H. sapiens* dPGM
Ce-2	Ac-DYDYPGDYCYLYGTCG (S–S)	8.65	8.27	7.72	8.21	8.78	NA	NA
Ce-2S	Ac-DYDYPGDYCYLYGTSG (S–S)	8.08	6.28	5.99	6.01	8.00	NA	NA
Ce-2-D1	Ac-DYDYPGDHCYLYGT(X) (S–S)	7.1	6.92	5.82	6.52	6.95	NA	NA
Ce-2-D2	Ac-DYDYPGDHCYLYG(X) (S–S)	7.0	6.06	5.95	6.64	7.0	NA	NA

pIC_{50} = -log IC_{50}, ex. pIC_{50}=9 equal IC_{50}=10^{-9} M. NA = No appreciable inhibitory activity at highest concentration tested. X = DOPA

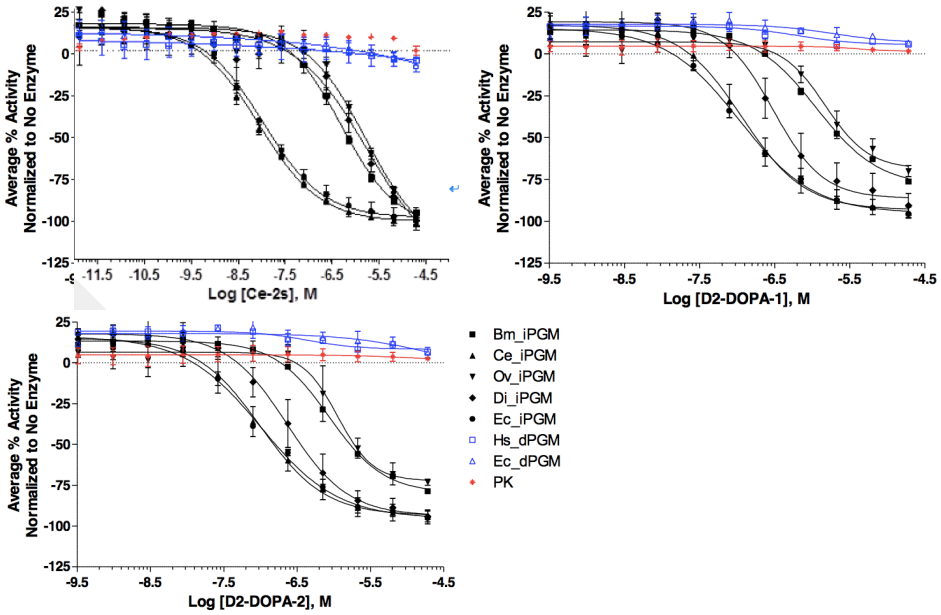

Figure 3-7. IC_{50} concentration-response curves for characterization of Ce-2S, Ce-2D1 and Ce-2D2 on the iPGM orthologs and dPGM isozymes using the enzyme coupled bioluminescent assay.

3.2.3.3 N-methyl scanning analysis of tail peptide of Ce-2

N-methylated amino acids were found in many biologically active natural products.[9] *N*-methylation of peptide backbone exhibit the ability to improve drug-like properties of peptides such as enhanced potency, target selectivity, membrane permeability and enzymatic stability. *N*-methylation on peptide backbone has been proved as a powerful structural modification approach to study biological activity of peptides.[10]

Since the C-terminal region of Ce-2 is critical for binding affinity and inhibitory function, with the aim of studying the structure activity relationship in this region, I decided to modify the backbone of Ce-2 C-terminal with *N*-methylations, and thus synthesized a series of *N*-methylated peptides.[11,12] The binding affinities of *N*-methylated analogs were tested by SPR analysis and showed in Table 3-10.

The set of single *N*-methylated Ce-2 peptides was tested for their ability to bind *C. elegans* iPGM and compared with the native Ce-2, which acted as a positive control. Increased dissociation rates (k_d) were detected for the peptides Ce-2a, Ce-2b, Ce-2c and Ce-2d, which resulted in lost of binding affinity to *C. elegans* iPGM, indicating that the additional methyl group might affect the conformation of Ce-2 and negatively affect binding ability. For the peptides Ce-2e and Ce-2f, slightly enhanced binding was detected, with the dissociation constants (K_D) were 7 fold lower than Ce-2, implying that extra methyl groups contribute to the interaction with target protein. Ce-2g exhibited similar binding affinity to parent peptide Ce-2, implying that C-terminal glycine residue rarely contributes to intra and inter molecular interaction.

Since binding affinity of Ce-2 was improved by single methylation on T13, C14 and G15 residues, we concerned that whether multiple *N*-methylations would further enhance its activity. To explore this question, I prepared di and tri N-methylated peptides, Ce-2h, Ce-2i, Ce-2j and Ce-2k and examined binding activities of these analogs (Table 3-10). Generally, The di N-methylated peptides displayed slightly enhanced binding affinity than parent Ce-2 and single *N*-methylated analogs. The binding activity of tri N-methylated analog Ce-2k was lower than Ce-2 as result of increased dissociation rate (k_d).

Table 3-10. The binding affinities of N-methylated Ce-2 peptide analogs against *C. elegans* iPGM.

Peptide ID	Sequence	k_a ($\times 10^6$ $M^{-1}s^{-1}$)	k_d ($\times 10^{-3}$ s^{-1})	K_D (nM)
Ce-2	Ac-D-Y(X)C-S-CYLYGTCG	2.69	1.31	4.9
Ce-2a	Ac-D-Y(X)C-S-C^{Me}YLYGTCG	1.85	7.18	38.9
Ce-2b	Ac-D-Y(X)C-S-CY^{Me}LYGTCG	4.54	30.9	68.0
Ce-2c	Ac-D-Y(X)C-S-CYL^{Me}YGTCG	3.04	48.7	16.0
Ce-2d	Ac-D-Y(X)C-S-CYLY^{Me}GTCG	0.86	15.8	18.3
Ce-2e	Ac-D-Y(X)C-S-CYLYG^{Me}TCG	2.33	1.44	0.61
Ce-2f	Ac-D-Y(X)C-S-CYLYGT^{Me}CG	2.32	1.56	0.67
Ce-2g	Ac-D-Y(X)C-S-CYLYGTC^{Me}G	0.41	1.94	4.7
Ce-2h	Ac-D-Y(X)C-S-CYLYGT^{Me}C^{Me}G	2.64	2.36	0.89
Ce-2i	Ac-D-Y(X)C-S-CYLYG^{Me}TC^{Me}G	1.15	2.69	2.3
Ce-2j	Ac-D-Y(X)C-S-CYLYG^{Me}T^{Me}CG	0.96	3.67	3.8
Ce-2k	Ac-D-Y(X)C-S-CYLYG^{Me}T^{Me}C^{Me}G	0.26	2.06	8.0

X represents DYPGDY sequence

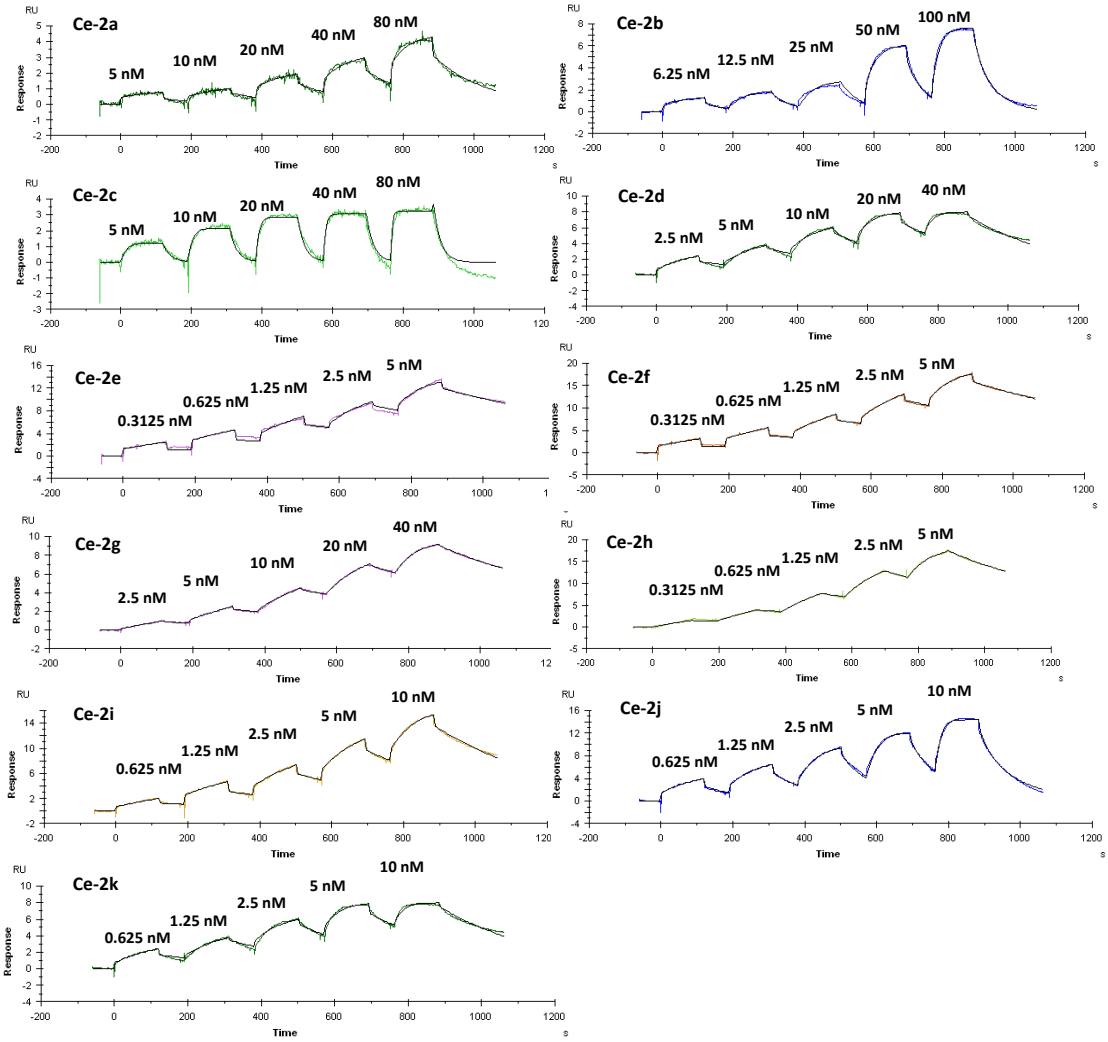

Figure 3-8. SPR sensorgrams of truncated *N*-methylated Ce-2 analogs against *C. elegans* iPGM measured by the Biacore T100 instrument. The measurements were performed by single-cycle kinetic mode with five peptide concentrations.

The effect of backbone *N*-methylation on inhibitory activity was also determined (Table 3-11). Single *N*-methylation of Tyr9 (Ce-2a), Leu10 (Ce-2b) and Gly12 (Ce-2d) reduced the inhibitory potency dramatically, and negatively impact on the broad-spectrum inhibitory activity, implying that backbones of these residues contribute to inhibitory activity and the additional methyl groups could hinder the formation of active structure and interrupt peptide-protein interactions. *N*-methylation of Tyr11 (Ce-2c), Thr13 (Ce-2e), Cys14 (Ce-2f) and Gly15 (Ce-2g) retained the potency against *C. elegans* iPGM, but slightly impact on the broad-spectrum inhibitory activity, indicating that these positions were compatible with *N*-methylation and would improve biological property. Interestingly, multiple *N*-methylations had also retained the potency as single *N*-methylation.

Table 3-11. The inhibitory activity of *N*-methylated analogs against target enzyme *C. elegans* iPGM and four iPGM orthologs from *B. malayi*, *O. volvulus*, *D. immitis* and *E. coli*, two PGM isozyme from *E. coli* and *H. sapiens*

Peptide ID	Sequence	pIC_{50}						
		B. malayi iPGM	*C. elegans* iPGM	*O. volvulus* iPGM	*D. immitis* iPGM	*E. coli* iPGM	*E. coli* dPGM	*H. sapiens* dPGM
Ce-2	Ac-D-Y(X)CYLYGTCG	8.27	8.65	7.72	8.21	8.78	NA	NA
Ce-2a	Ac-D-Y(X)C^{Me}YLYGTCG	NA	5.05	NA	NA	5.05	NA	NA
Ce-2b	Ac-D-Y(X)CY^{Me}LYGTCG	5.25	5	NA	5.25	NA	NA	NA
Ce-2c	Ac-D-Y(X)CYL^{Me}YGTCG	7	8	6.35	6.8	8.2	NA	NA
Ce-2d	Ac-D-Y(X)CYLY^{Me}GTCG	5.4	6.2	5.05	5.4	6.4	NA	NA
Ce-2e	Ac-D-Y(X)CYLYG^{Me}TCG	7.95	8.5	7.15	7.75	8.65	NA	NA
Ce-2f	Ac-D-Y(X)CYLYGT^{Me}CG	7.8	8.2	6.95	7.6	8.45	NA	NA
Ce-2g	Ac-D-Y(X)CYLYGTC^{Me}G	7.91	8.46	7.11	7.63	8.67	NA	NA
Ce-2h	Ac-D-Y(X)CYLYGT^{Me}C^{Me}G	7.35	7.88	6.6	7.01	8.12	NA	NA
Ce-2i	Ac-D-Y(X)CYLYG^{Me}TC^{Me}G	7.43	8.19	6.67	7.08	8.51	NA	NA
Ce-2j	Ac-D-Y(X)CYLYG^{Me}T^{Me}CG	7.84	8.51	7.08	7.57	8.61	NA	NA
Ce-2k	Ac-D-Y(X)CYLYG^{Me}T^{Me}C^{Me}G	7.95	8.39	7.22	7.72	8.55	NA	NA

pIC_{50} = -log IC_{50}, ex. pIC_{50}=9 equal IC_{50}=10^{-9} M. NA = No appreciable inhibitory activity at highest concentration tested.

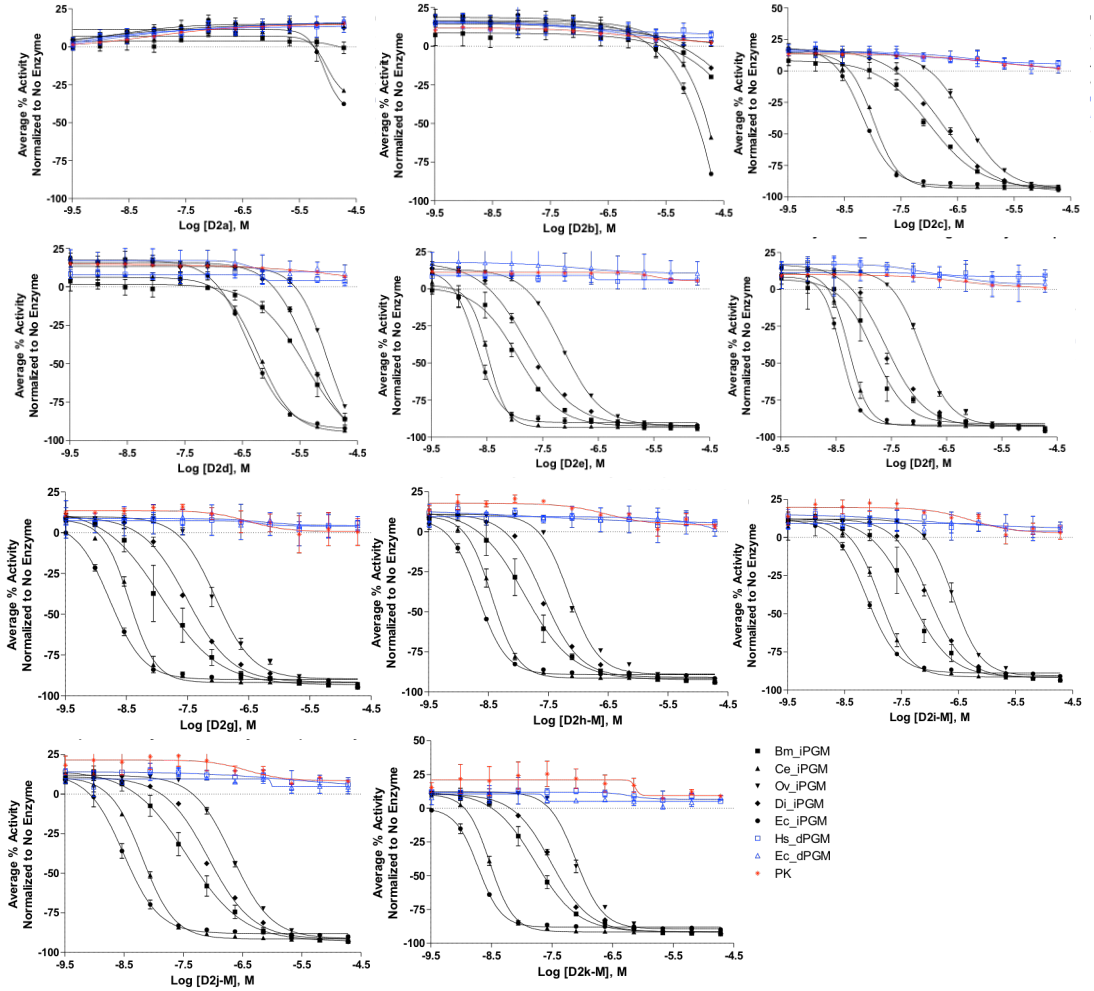

Figure 3-9. IC_{50} concentration-response curves for characterization of *N*-methylated Ce-2 analogs on the iPGM orthologs and dPGM isozymes using the enzyme coupled bioluminescent assay.

3.2.4 Co-crystal structure of iPGM Ce-2complex and inhibitory mechanism

The iPGM are monomeric enzymes comprising a phosphatase domain and phosphotransferase domain.[7,13] The X-ray crystal structures of iPGMs have been resolved to date, including enzymes derived from parasite and bacterial species.[14-16] However, The crystal structure of *C. elegans* iPGM has not been resolved until now. Structure activity relationship studies on the most potent peptide Ce-2 suggested that the tail peptide were key residues for inhibitory property. To investigate the inhibitory mechanism, we attempt to develop a structural model by co-crystallization of iPGM and peptide complex to represent the molecular interactions between peptide inhibitors and *C. elegans* iPGM.

3.2.4.1 Crystal structure of *apo C. elegans* iPGM

Macrocyclic peptide Ce-2 showed strong binding affinity and highest inhibitory activity toward *C. elagans* iPGM. It was chosen to resolve the co-crystal structure with *C. elegans* iPGM. Although it was failed to obtain a complex crystal structure, The crystal structure of *apo C. elegans* iPGM (magenta) was solved successfully, which was the first crystal structure of a nematode iPGM (Figure 3-10). The model of *C. elegans* iPGM consisted of two domains conjugating by loop sequence. Each domain consists of central β-sheet array α-helices. Phosphotransferase domain contains the active site for substrate binding, while phosphatase domain harbors the catalytic site with two metal ions coordinated by catalytic residues (Figure 3-10). The Zn^{2+} ion coordinated with Asp37, Ser86, Asp467 and His468 in a tetrahedral manner. The other Mn^{2+} ion is coordinated with Asp426, His430 and His485.

The *apo C. elegans* iPGM (magenta) was compared with *apo Bacillus anthracis* iPGM (cyan, PDB: 2IFY) a well studied iPGM ortholog via superposition and yielded an RMSD of 2.76 Å between Cα atoms (476 residues aligned). The overall structure is very similar without significant deviation. The two catalytic domains and metal binding site are quite similar.

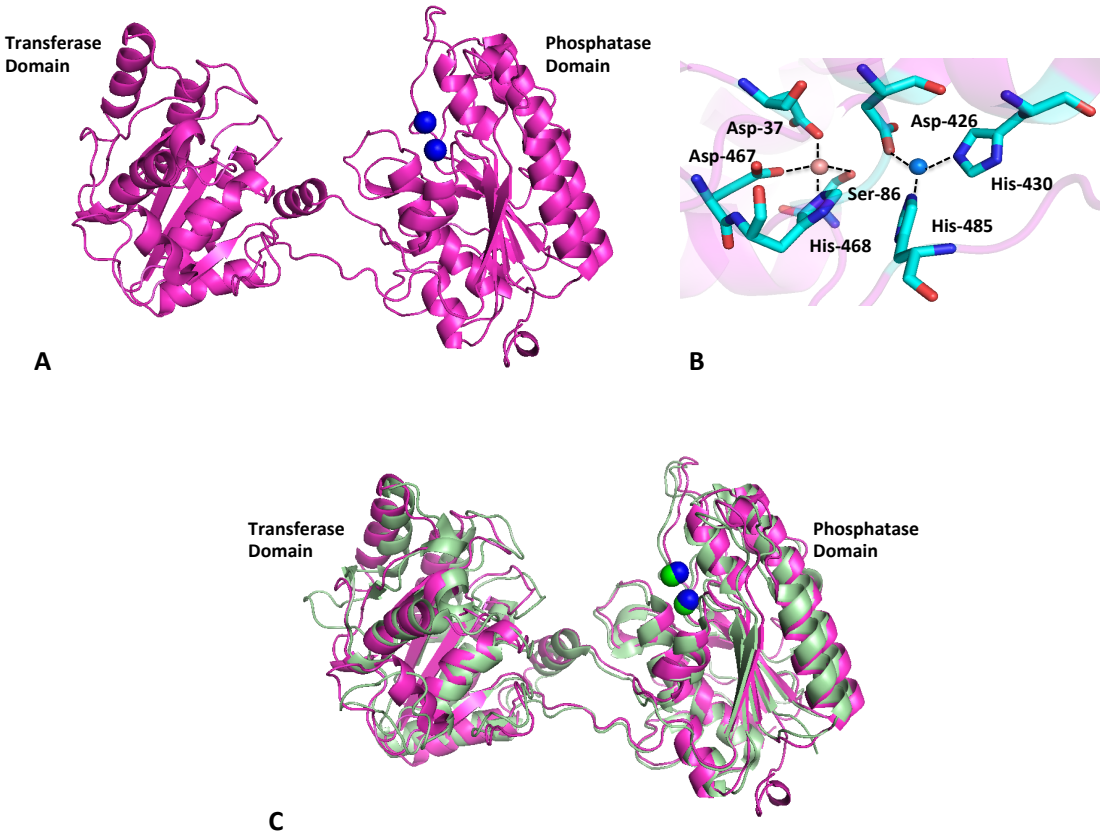

Figure 3-10. Crystal structure of *apo C. elegans* iPGM (magenta), the coordinate geometry of metal ions and comparison of *C. elegans* iPGM to *apo Bacillus anthracis* iPGM (cyan), PDB: 2IFY

3.2.4.2 Co-crystal structure of *C. elegans* iPGM-Ce-2d complex and locked-open inhibitory mechanism

Crystallization of peptide enzyme complex was retried using a *N*-terminal truncated analog Ce-2-4 that exhibits similar bind and inhibitory activity as Ce-2 against *C. elegans* iPGM. The preformed complex of peptide and enzyme was purified by sizing chromatography. Co-crystal was obtained by incubating iPGM with Ce-2-4 at a ratio of 1:1.5. This incubation resulted in needle like crystal, which was diffracted to 1.95 Å. The final analysis generates iPGM-Ce2-4 model in which two asymmetric units were obtained. In this model, Ce-2-4 was bounding to *C. elegans* iPGM in a compact manner and occupying a pocket formed by hinge peptides between phosphatase domain and phosphotransferase domain (Figure 3-11).

In order to investigate the conformational changes, superposition of *apo C. elegans* iPGM and Ce-2-4 and *C. elegans* iPGM complex was conducted (Figure 3-11). and yielded an RMSD deviation of 1.98 Å. The overall structure are remarkably similar, the conformation of binding pocket in complex had slightly changed to accommodate the peptide. The peptide fit within the pocket in an optimized conformation, which might be endowed by affinity selection in the discovery of parent peptides. Since iPGM undergo open-closed-open conformational change during catalytic cycles, the enzyme was trapped at its open state by the peptide macrocycle, thus a locked-open inhibition mechanism was illuminated, indicating an possible insight for novel inhibitor discovery by blocking the enzyme in open conformation.

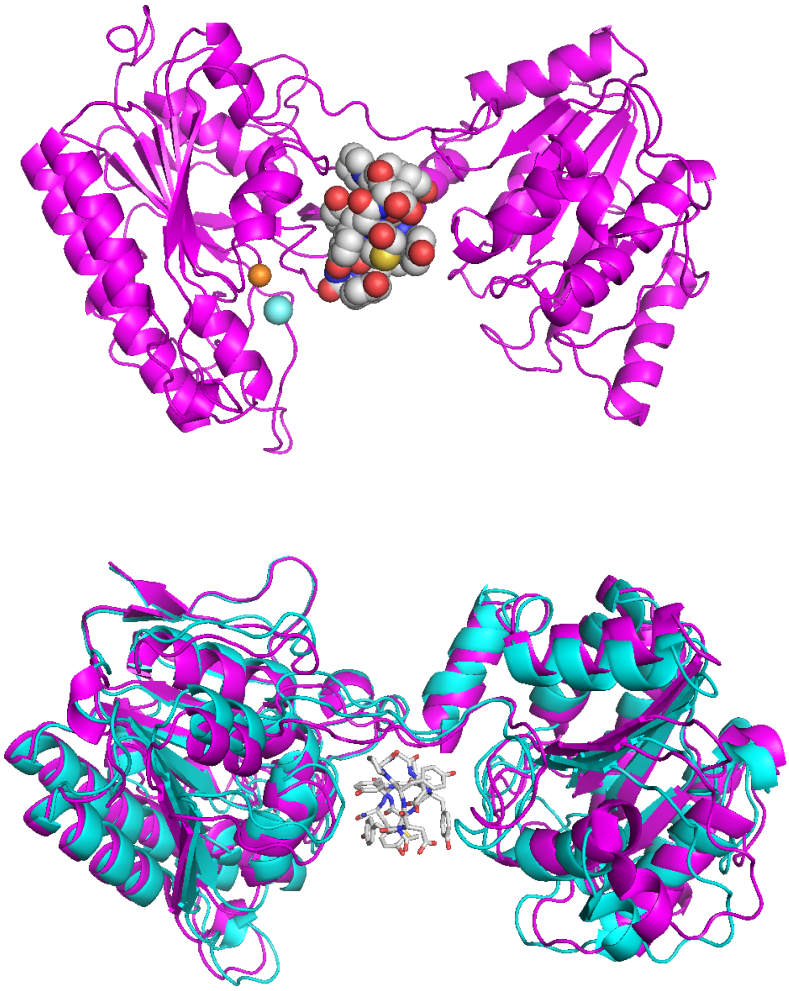

Figure 3-11. Crystal structure of *C. elegans* iPGM (magenta) with Ce-2-4 and comparison of *C. elegans* iPGM complex to *apo C. elegans* iPGM (cyan)

3.2.4.3 The interaction between Ce-2-4 and *C. elegans* iPGM

The Ce-2-4 has been identified as tight iPGM binder with K_D value of 1.9 nM. The analysis of co-crystal complex displayed that Ce-2-4 bound to *C. elegans* iPGM via multiple interactions, including hydrogen bonds, hydrophobic and water mediate interaction (Figure 3-12). Sidechains of Asp2 and Tyr3 in Ce-2-4 are shown to be hydrogen bonding with residues Arg289 and Asp102 of *C. elegans* iPGM, respectively. Carbonyl group of Gly5 is hydrogen bonding with Asp102 and Asn101 sidechain. Asn85 sidechain interacted with Carbonyl group of Tyr9 via hydrogen bond. C-terminal Tyr11 made a hydrogen bond with carboxyl group of Glu87. Leu10 side chain positioned in a pocket seems to be taking part in hydrophobic interactions with side chains of Leu78, Leu82 and Ile103.

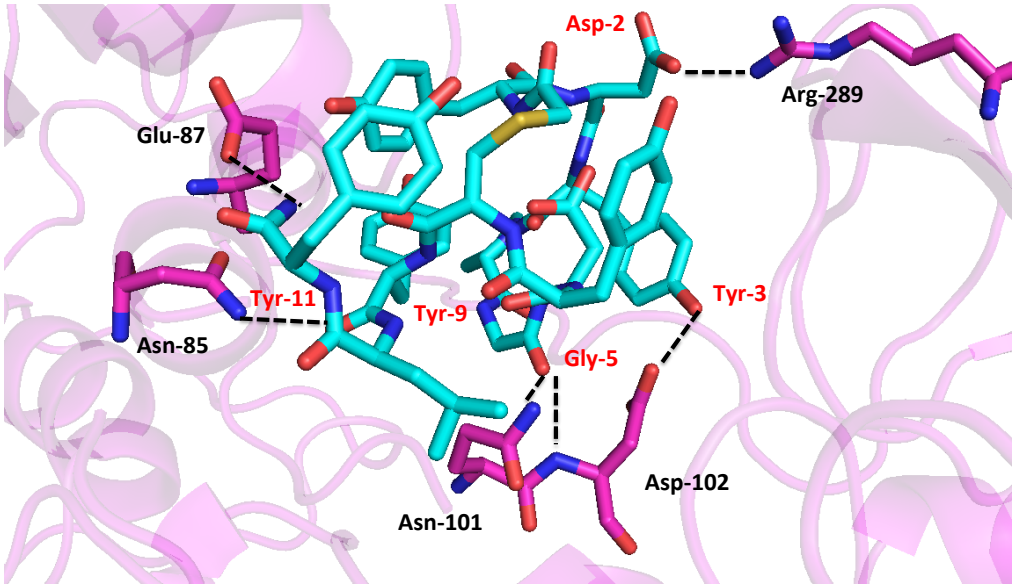

Figure 3-12. The interactions between Ce-2-4 (backbone in cyan) and *C. elegans* iPGM residues (in magenta).

3.2.4.4 The active conformation of Ce-2-4 in complex

Ce-2-4 comprises of 11 amino acids and lariat-like structure, form a cyclic head of 8 amino acids with linear tail containing 3 amino acids. In the co-crystal structure, the Ce-2-4 was bounding between the two domains of *C. elegans* iPGM and at a compact conformation (Figure 3-13).

The side chains of amino acid residues in the cyclic head directed outward, except Asp6 side chain, which direct to the center of cyclic circle. The carboxyl group of Asp6 interacts with four backbone amide hydrogens, an extra hydrogen bond formed between Tyr3 hydroxyl and Asp6 amide group in the backbone. These intra cyclic interactions keep the peptide in constrained backbone conformation.

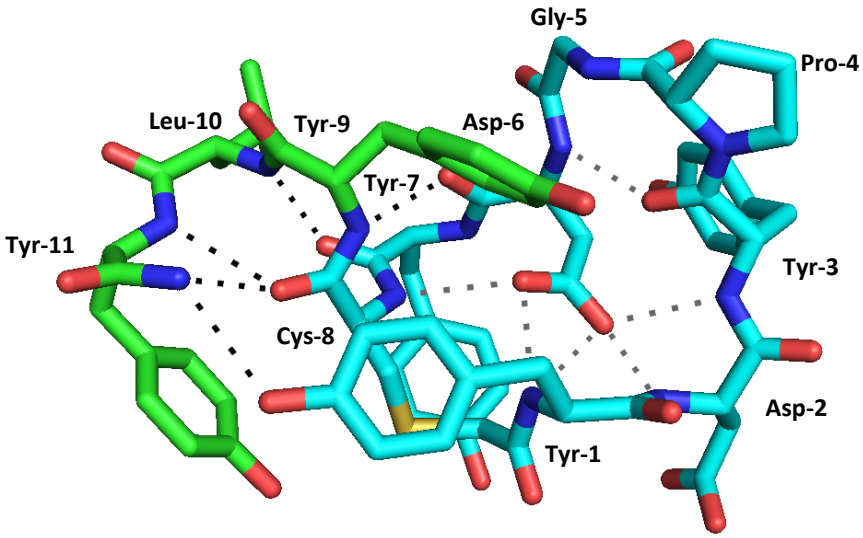

Figure 3-13. The conformation of Ce-2d and intermolecular interactions. The cyclic head and linear tail are colored in cyan and green, respectively.

The peptide structure is further stabilized by a α-helix conformation by forming hydrogen bonds between the amide group of Leu10/Tyr11 and carbonyl group of Tyr7/Cys8. The interaction between hydroxyl group of Tyr1 and N-terminal amide of Tyr11 as well as assists the formation of compact active structure. This observation suggests that the N-methylation on Tyr9 and Leu10 might hinder the formation of hydrogen bonds that lead to the negative effect on inhibitory activity of Ce-2 peptide,

in aforementioned structure activity relationship studies. Moreover, the C-terminal residues of Tyr9, Leu10 and Tyr11 are pointing toward the metal ion active site. The longer C-terminus of Ce-2 could position Cys14 within coordination distance to the metal ions.

3.2.4.5 Modeling of C-terminal truncated residues of Ce-2 onto Ce-2-4

Since the co-crystal structure of Ce-2 and *C. elegans* iPGM has not been obtained. To obtain more insight of binding mechanism of Ce-2 to *C. elegans* iPGM, Gly12-Thr13-Cys14-Gly15 residues were modeled onto complex of Ce-2-4 and iPGM (Figure 3-14). This was a collaboration work with NIH. This modeling positions the Cys14 within coordination distance of Mn^{2+}, which plays key role in iPGM catalytic property. Based on this model, we assume that Cys14 side chain could coordinately interplay with Mn^{2+} ion and interrupt the original coordinate interactions between Mn^{2+} ion and catalytic residues. The result of this modeling suggest that the coordinative interaction between metal ion and Cys14 sidechain might act together with peptide-iPGM interaction to maintain potent and broad-spectrum inhibitory activity against iPGMs.

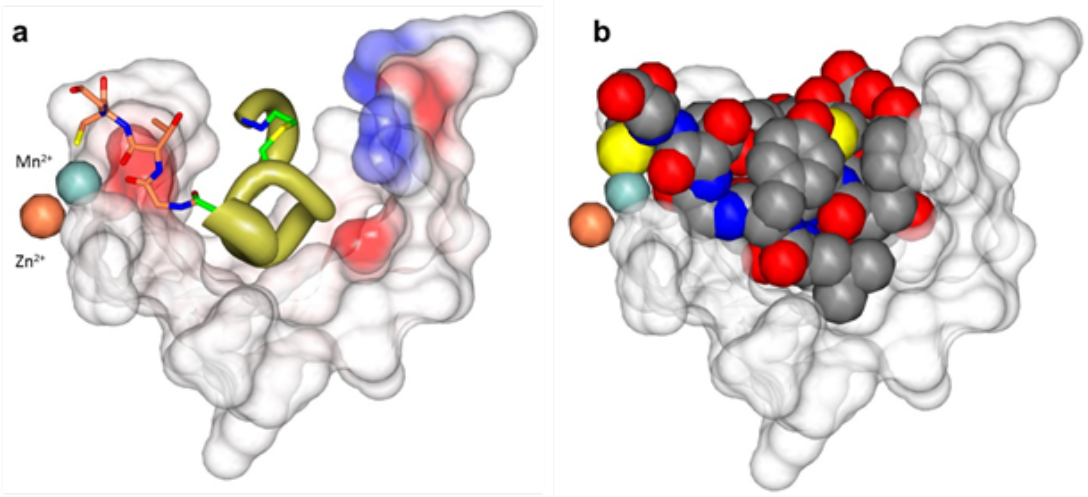

Figure 3-14. Modeling of C-terminal residues of Ce-2 onto Ce-2-4. (a) the C-terminal residues of Gly12-Thr13-Cys14-Gly15 are shown as tan sticks extending from Ce-2d. (b) The Ce-2 is shown in sphere model. The sulfhydryl group of Cys 14 is shown in yellow. The Mn2+ and Zn2+ ions are shown as blue and tan spheres, respectively.

3.3 Conclusion

In this chapter, I reported the discovery of macrocyclic peptide inhibitors against *C. elegans* iPGM using the RaPID system. Four macrocyclic peptides were isolated via *in vitro* affinity selection. Ce-1 and Ce-2 are lariat-like peptides with cyclic head and linear tail. Ce-3 and Ce-4 are macrocyclic peptide. The binding affinity and inhibitory activity of peptides were determined by SPR analysis and inhibition assays. All selected peptides exhibit high binding ability toward *C. elegans* iPGM. Ce-1 and Ce-2 displayed potent and broad-spectrum inhibitory activity against iPGM orthologs and selectivity toward dPGM. Ce-2 is the most potent iPGM inhibitor against iPGM orthologs (pIC_{50} = 7.72-8.65, IC_{50} = 2.2-19 nM).

Structure activity relationship studies were extensively performed with Ce-2. Truncation and *N*-methylation scanning studies on Ce-2 demonstrated that the cyclic head are essential structure for binding ability and tail peptide residues, C-terminal cysteine-14 are involving broad-spectrum inhibitory property.

Furthermore, the crystal structure of *apo C. elegans* iPGM was solved for the first time. The co-crystal structure of peptide and *C. elegans* iPGM was also obtained. The macrocyclic peptide bound to *C. elegans* iPGM in compact manner between phosphatase domain and phosphotransferase domain and trapped the iPGM enzyme at open state. This observation elucidated a locked-open inhibitory mechanism. The molecular and crystallographic information would facilitate the development and rational design of anti-parasite therapeutics.

3.4 Materials and experimental section

3.4.1 Materials

All reagents used were as the same as described in Chapter 2. Fmoc-L-Lys(Mmt)-OH and Fmoc-βAla-OH were purchased from Merck Millipore and Watanabe Chemical Industries, respectively. Fluorescein-NHS and Fmoc-DOPA was purchased from Thermo Scientific.

3.4.2 Aminoacylation of tRNAs assisted by eFx

eFx was mixed with $tRNA^{fMet}_{CAU}$ to a final concentration of 25μM in 50 mM HEPES-KOH (pH 7.5) with 600 mM $MgCl_2$. This mixture was heated at 95 °C for 2 min, stand at room temperature for 5 min and incubated on ice for another 5 min. Then home made N-chloroacetyl D-Tyrosine cyanomethyl ester or N-chloroacetyl L-Tyrosine cyanomethyl ester dissolved in DMSO was added to a final concentration of 5 mM and incubated one more hour on ice. Then 0.3M sodium acetate (pH5.2) was added to quench the acylation reaction. The acylated tRNA product was participated and purified by ethanol and the final pellet was dried and dissolved in 1.0 μL of 0.1 mM sodium acetate.

3.4.4 Chemical synthesis and purification of parent peptides and analogs

All peptides were synthesized using Fmoc-based SPPS via Syro Wave automated peptide synthesizer (Biotage) in the same manner as described in Chapter 2. A acetyl group was coupled on to the N-terminal amide group for the formation of linear peptides after the automated synthesis. *N*-methylated amino acid containing analogs were manually synthesized referring to procedures described in this protocol. [11] Then peptides were purified by reverse-phase HPLC (RP-HPLC), molecular masses were verified by MALDI-TOF mass spectrometry, using a microflex or ultraflex instrument (Bruker Daltonics).

3.4.5 Surface plasmon resonance (SPR) analysis

Biacore T100 instrument (T200 sensitivity enhanced) was used to evaluate the binding affinity of peptides against C. elegans iPGM. Dissociation constants were determined using single cycle kinetic analysis. *C. elegans* iPGM (His_{10} tagged) was immobilized on a NTA sensor chip (GE Healthcare) as ligand. HBS-P solution containing 0.1% DMSO was used as running buffer. 200 nM C. elegans iPGM was immobilized on sensor chip in running buffer at 10 μL/min. Peptides were runned over the sensor chip as analyte with five concentrations between 1 and 1000 nM. The Dissociation constants of each peptide were determined by repeat the process with optimized concentration.

3.4.6 Size exclusion chromatography

Samples of peptide and iPGM complex were analyzed on a Superdex 75 16/600 column using an AKTA Pure system before crystallization. 500 μL sample was applied to the column and eluted at 1 mL/min with buffer containing 30mM Tris, 150 mM NaCl and 2 mM $MgSO_4$. Eluted samples were monitored at 280 and 500 nm and collected in 96 deep-well plates.

3.4.7 Crystallization and data collection

iPGM from *Caenorhabditis elegans* was prepared at a concentration of 10.8 mg/mL in 150 mM NaCl, 30 mM Tris pH 8.0 for crystallization screening. Ce-2d was prepared in DMSO at a concentration of 50 mM and mixed with iPGM in a 1:1.5 (protein: cyclic peptide) molar ratio. The mixture was incubated on ice for 30 minutes. Apo iPGM: two forms of crystal were obtained from Crystal Screen HT (Hampton Research) and transferred to 75% crystallization solution and 25% PEG 400. iPGM-Ce-2d complex: needle-like crystal were obtained after 7 days of Crystal Screen HT (Hampton Research) and transferred to 80% crystallization solution and 20% glycerol. All the samples were stored in liquid nitrogen. X-ray diffraction data were collected using a Dectris Pilatus 6M pixel array detector.

3.4.8 The chemical structure and MSMS spectrum of Ce-2

The chemical structure of Ce-2 peptide is showed below.

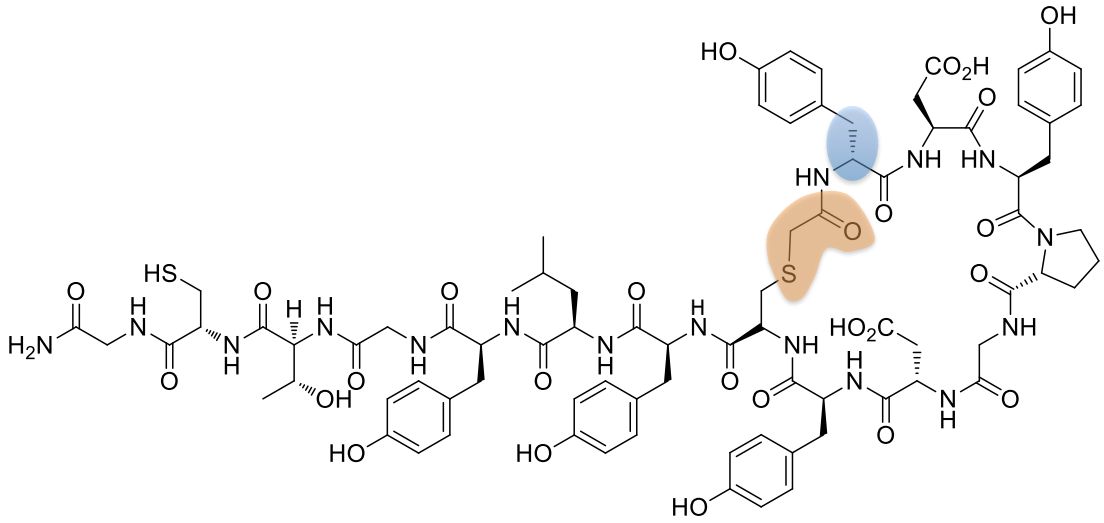

Figure 3-15. The structure of Ce-2 macrocyclic peptide

Macrocyclic peptide Ce-2 was analyzed by MALDI-TOF/TOF. b-type, y-type and c-type fragment ions were indicated by number. The parent ion [M+H]+ of Ce-2 is 1790.66.

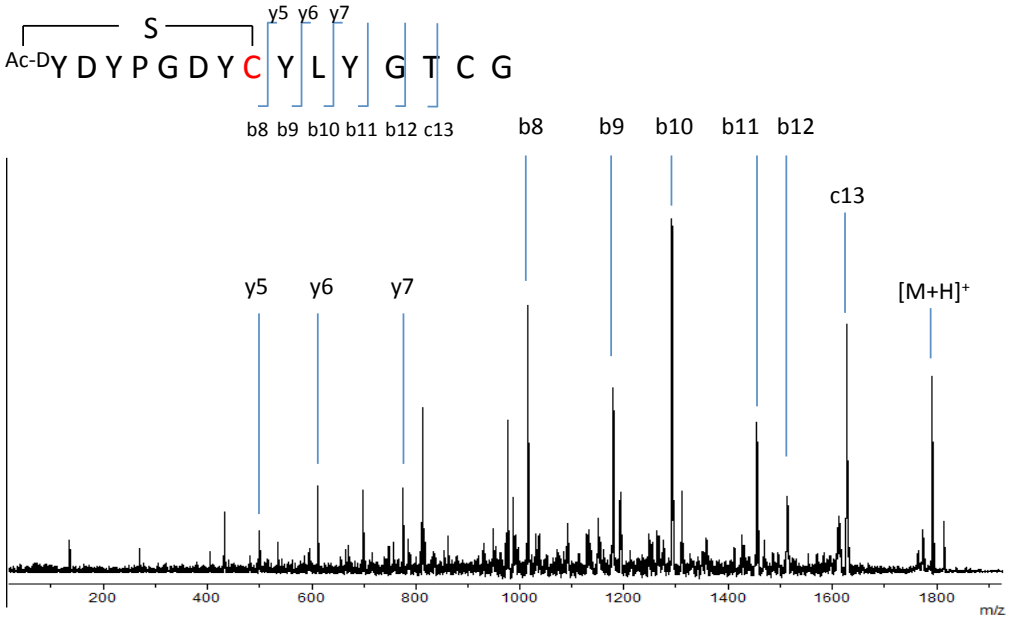

Figure 3-16. The MSMS spectrum of Ce-2 macrocyclic peptide

3.5 References

1 Brenner, S. The genetics of Caenorhabditis elegans. *Genetics* **77**, 71-94 (1974).

2 Wood, W. B. The nematode Caenorhabditis elegans (Cold Spring Harbor New York, 1988).

3 Hengartner, M. O. & Horvitz, H. R. The ins and outs of programmed cell death during C. elegans development. *Philosophical Transactions of the Royal Society of London B: Biological Sciences* **345**, 243-246 (1994).

4 Hengartner, M. O. & Horvitz, H. R. Programmed cell death in Caenorhabditis elegans. *Current opinion in genetics & development* **4**, 581-586 (1994).

5 Kenyon, C., Chang, J., Gensch, E., Rudner, A. & Tabtiang, R. A C. elegans mutant that lives twice as long as wild type. *Nature* **366**, 461-464 (1993).

6 Fire, A. *et al.* Potent and specific genetic interference by double-stranded RNA in Caenorhabditis elegans. *Nature* **391**, 806-811 (1998).

7 Jedrzejas, M. J., Chander, M., Setlow, P. & Krishnasamy, G. Mechanism of Catalysis of the Cofactor-independent Phosphoglycerate Mutase from Bacillus stearothermophilus Crystal structure of the complex with 2-phosphoglycerate. *Journal of Biological Chemistry* **275**, 23146-23153 (2000).

8 Zhang, Y., Foster, J. M., Kumar, S., Fougere, M. & Carlow, C. K. S. Cofactor-independent phosphoglycerate mutase has an essential role in Caenorhabditis elegans and is conserved in parasitic nematodes. *Journal of Biological Chemistry* **279**, 37185-37190 (2004).

9 Chatterjee, J., Gilon, C., Hoffman, A. & Kessler, H. N-methylation of peptides: a new perspective in medicinal chemistry. *Accounts of chemical research* **41**, 1331-1342 (2008).

10 Chatterjee, J., Rechenmacher, F. & Kessler, H. N‐Methylation of Peptides and Proteins: An Important Element for Modulating Biological Functions. *Angewandte Chemie International Edition* **52**, 254-269 (2013).

11 Chatterjee, J., Laufer, B. & Kessler, H. Synthesis of N-methylated cyclic peptides. *Nature protocols* **7**, 432-444 (2012).

12 Miller, S. C. & Scanlan, T. S. Site-selective N-methylation of peptides on solid support. *Journal of the American Chemical Society* **119**, 2301-2302 (1997).

13 Jedrzejas, M. J., Chander, M., Setlow, P. & Krishnasamy, G. Structure and mechanism of action of a novel phosphoglycerate mutase from Bacillus stearothermophilus. *The EMBO journal* **19**, 1419-1431 (2000).

14 Nukui, M. *et al.* Structure and molecular mechanism of Bacillus anthracis cofactor-independent phosphoglycerate mutase: a crucial enzyme for spores and growing cells of Bacillus species. *Biophysical journal* **92**, 977-988 (2007).

15 Mercaldi, G. F., Pereira, H. M., Cordeiro, A. T., Michels, P. A. M. & Thiemann, O. H. Structural role of the active‐site metal in the conformation of Trypanosoma brucei phosphoglycerate mutase. *FEBS Journal* **279** (2012).

16 Roychowdhury, A. *et al.* Complete catalytic cycle of cofactor‐independent phosphoglycerate mutase involves a spring‐loaded mechanism. *FEBS journal* **282**, 1097-1110 (2015).

Chapter 4
General conclusion

4.1 General conclusion

In this thesis, I have reported the development of macrocyclic peptide inhibitors against iPGMs via *in vitro* affinity selection by means of the RaPID system. The selection toward *B. malayi* iPGM generated macrocyclic peptide with inhibitory activity. Several macrocyclic peptides with high binding affinity were discovered successfully by performing selection against *C. elegans* iPGM. Selected peptide candidates showed inhibitory activity toward iPGM enzyme and are potent inhibitors against iPGM orthologs. To the best of our knowledge, the macrocyclic peptides reported here represent the first peptide macrocycles with potent inhibitory activity against iPGMs and isozyme-selectivity against dPGM and could be promising drug lead for the development of anti-parasite therapeutics.[1-6]

Furthermore, extensive structure activity relationship studies on Ce-2 demonstrated the importance of tail peptide and C-terminal cysteine for maintaining potent inhibitory ability. The binding site of macrocyclic peptide was presented by obtained co-crystal structure of peptide-iPGM complex. The cyclic peptide bound in compact manner between interface of two catalytic domains, which undergo open-closed-open conformational change for one catalytic cycle.[7] The enzyme was trapped at its open state by the peptide macrocycle, this binding model illuminated an open-locked inhibition mechanism.

The discoveries in this thesis demonstrated that macrocyclic peptides are alternative compound class for developing novel therapeutic agents against targets that could not be modulated by small molecules. The RaPID system had been proved to be a powerful and productive approach to discover peptide macrocycles targeting otherwise undruggable targets. The structure studies and binding model analysis provide insights for the future study and optimization of iPGM inhibitors. The inhibitory mechanism information discussed here would stimulate the development of novel antimicrobials agents and rational drug design.

4.2 References

1 WHO. *Weekly epidemiological record*. Vol. 35 377-388 (2011).

2 Fischer, P., Supali, T. & Maizels, R. M. Lymphatic filariasis and Brugia timori: prospects for elimination. *Trends in parasitology* **20**, 351-355 (2004).

3 Zhang, Y., Foster, J. M., Kumar, S., Fougere, M. & Carlow, C. K. S. Cofactor-independent phosphoglycerate mutase has an essential role in Caenorhabditis elegans and is conserved in parasitic nematodes. *Journal of Biological Chemistry* **279**, 37185-37190 (2004).

4 Kumar, S. *et al.* Mining predicted essential genes of Brugia malayi for nematode drug targets. *PloS one* **2**, e1189 (2007).

5 Singh, P. K., Kushwaha, S., Mohd, S., Pathak, M. & Misra-Bhattacharya, S. In vitro gene silencing of independent phosphoglycerate mutase (iPGM) in the filarial parasite Brugia malayi. *Infectious Diseases of Poverty* **2**, 1 (2013).

6 Crowther, G. J. *et al.* Cofactor-independent phosphoglycerate mutase from nematodes has limited druggability, as revealed by two high-throughput screens. *PLoS Negl Trop Dis* **8**, e2628 (2014).

7 Roychowdhury, A. *et al.* Complete catalytic cycle of cofactor‐independent phosphoglycerate mutase involves a spring‐loaded mechanism. *FEBS journal* **282**, 1097-1110 (2015).

List of accomplishment

Paper

1. Hao Yu, Patricia Dranchak, James Inglese, Hiroaki Suga
   Potent macrocyclic peptide inhibitors against cofactor-independent phosphoglycerate mutase.
   PEPTIDE SCIENCE 2015, 2016, 345-346.

Acknowledgment

It has been a great experience to study the University of Tokyo and memorable times to work in Suga laboratory with all members.

I greatly appreciate Prof. Hiroaki Suga for his constant support and insightful supervision. He taught me so much on scientific thinking and ideas and encouraged me to overcome difficulties.

I also would like to acknowledge Associate Professor Nakazu Kano who gave me suggestions on presentation skills and Assistant Professor Takayuki Katoh, Assistant Professor Yuki Goto and Assistant Professor Toby Passioura for all of their everyday guidance. I also would like to thank lab members for their constant and patient help.

I really appreciate Prof. James Inglese and Dr. Patricia Dranchak from National institutes of health with collaboration works of biological assays as well as protein crystallography analysis.

Lastly, I would like to thank my family members and friends for their lovely support and kind encouragement.

Hao Yu